Accepted Manuscript

Machine learning prioritizes synthesis of primaquine ureidoamides with high antimalarial activity and attenuated cytotoxicity

Jurica Levatić, Kristina Pavić, Ivana Perković, Lidija Uzelac, Katja Ester, Marijeta Kralj, Marcel Kaiser, Matthias Rottmann, Fran Supek, Branka Zorc

PII: S0223-5234(18)30075-8

DOI: 10.1016/j.ejmech.2018.01.062

Reference: EJMECH 10139

To appear in: *European Journal of Medicinal Chemistry*

Received Date: 16 November 2017

Revised Date: 16 January 2018

Accepted Date: 18 January 2018

Please cite this article as: J. Levatić, K. Pavić, I. Perković, L. Uzelac, K. Ester, M. Kralj, M. Kaiser, M. Rottmann, F. Supek, B. Zorc, Machine learning prioritizes synthesis of primaquine ureidoamides with high antimalarial activity and attenuated cytotoxicity, *European Journal of Medicinal Chemistry* (2018), doi: 10.1016/j.ejmech.2018.01.062.

Machine learning prioritizes synthesis of primaquine ureidoamides with high antimalarial activity and attenuated cytotoxicity

Jurica Levatić [a,b], Kristina Pavić [c], Ivana Perković [c], Lidija Uzelac [d], Katja Ester [d], Marijeta Kralj [d], Marcel Kaiser [e], Matthias Rottmann [e], Fran Supek [a,*], Branka Zorc [c,*]

[a] *Genome Data Science, Institute for Research in Biomedicine (IRB Barcelona), The Barcelona Institute of Science and Technology (BIST). Baldiri Reixac 10, 08028, Barcelona, Spain*

[b] *Department of Knowledge Technologies, Jožef Stefan Institute, Jamova cesta 39, SI-1000, Ljubljana, Slovenia*[c] *Faculty of Pharmacy and Biochemistry, University of Zagreb, A. Kovačića 1, HR-10 000 Zagreb, Croatia*

[d] *Laboratory of Experimental Therapy, Division of Molecular Medicine, Rudjer Bošković Institute, Bijenička cesta 54, HR-10 000 Zagreb, Croatia*

[e] *Parasite Chemotherapy, Medical Parasitology & Infection Biology, Swiss Tropical and Public Health Institute, 4051 Basel, Switzerland*

* Corresponding authors.

E-mail addresses: fran.supek@irbbarcelona.org (F. Supek); bzorc@pharma.hr (B. Zorc).

A B S T R A C T

Primaquine (PQ) is a commonly used drug that can prevent the transmission of *Plasmodium falciparum* malaria, however its toxicity limits its use. We prepared five groups of PQ derivatives: amides **1a-k**, ureas **2a-k**, semicarbazides **3a,b**, acylsemicarbazides **4a-k** and *bis*-ureas **5a-v**, and evaluated them for antimalarial activity *in vitro* against the erythrocytic stage of *P. falciparum* NF54. Particular substituents, such as trityl (in **2j** and **5r**) and methoxybenzhydryl (in **3b** and **5v**) were associated with a favorable cytotoxicity-to-activity ratio. To systematically link structural features of PQ derivatives to antiplasmodial activity, we performed a quantitative-structure activity relationship (QSAR) study using the Support Vector Machines machine learning method. This yielded a highly accurate statistical model (R^2 = 0.776 in cross-validation), which was used to prioritize novel candidate compounds. Seven novel PQ-ureidoamides **10a-g** were synthesized and evaluated for activity, highlighting the benzhydryl ureidoamides **10e** and **10f** derived from *p*-chlorophenylglycine. Further experiments on human cell lines revealed that **10e** and **10f** are an order of magnitude less toxic than PQ *in vitro* while having antimalarial activity indistinguishable from PQ. The toxicity profile of novel compounds **10** toward human cells was particularly favorable when the glucose-6-phosphate dehydrogenase (G6PD) was inhibited, while toxicity of PQ was exacerbated by G6PD inhibition. Our work therefore highlights promising lead compounds for the development of effective antimalarial drugs that may also be safer for G6PD-deficient patients. In addition, we provide computational inference of antimalarial activity and cytotoxicity for thousands of PQ-like molecular structures.

Keywords: QSAR, Primaquine, Ureidoamide, Antimalarial activity, *Plasmodium falciparum*, Glucose-6-phosphate dehydrogenase

1. Introduction

Malaria is an infectious disease affecting humans and animals, caused by parasitic protozoans belonging to the genus *Plasmodium*. Of the five species that cause malaria in humans, *P. falciparum* is responsible for most malaria-associated mortality worldwide and is the predominant species in tropical and subtropical countries. The World Health Organization tracks a decline in the global malaria burden due to more efficient drugs and better mosquito control. However, malaria is still a life-threatening disease: in 2015 alone, there were an estimated 212 million new cases of malaria and 429 000 deaths [1].

Currently approved drugs include the artemisinins (artemisinin, dihydroartemisin, artemether, artesunate) and quinoline derivatives (chloroquine, amodiaquine, mefloquine, quinine and primaquine) [2]. Primaquine (PQ) is an 8-aminoquinoline antimalarial drug active against all species causing human malaria, including multi-resistant *P. falciparum* strains. PQ is the only clinically approved drug known to eliminate dormant liver forms of *P. ovale* and *P. vivax* [3]. In the case of *P. falciparum* malaria, PQ is uniquely effective in killing gametocytes produced during the sexual life stage of the parasite in the blood, disrupting the transmission of infection to mosquitoes and slowing the spread of the disease. This means that the biological activity profile of PQ (an 8-aminoquinoline) is different from standard 4-aminoquinoline antimalarial drugs such as chloroquine (CQ) or amodiaquine. In particular, CQ is active against the asexual blood stages (trophozoites) of *P. falciparum*, which feed on erythrocyte contents and therefore need to detoxify ingested heme, a process that CQ interferes with. In contrast, PQ is less effective against asexual blood stages of *P. falciparum*, but clears the sexual stage very efficiently. Therefore the

underlying molecular mechanism of action of PQ likely differs from CQ and related drugs, and is not currently well understood.

Because of the unique biological activity profile, PQ is complementary to other antimalarials and is commonly added to drug regimens, with the primary goal of containing the spread of malaria (in *P. falciparum*) or preventing relapse (for species with dormant liver stages, *P. ovale* and *P. vivax*). However, toxicity of PQ is an important concern [4], particularly in patients with a deficiency in the glucose-6-phosphate dehydrogenase (G6PD) enzyme – a widespread genetic trait, particulary in disease-endemic regions. Globally 400 million people are estimated to be affected with G6PD deficiency [5]. The highest prevalence is found in tropical Africa and tropical/subtropical Asia: approx. 5-30%, depending on the country and the method used to estimate the deficiency, reviewed in [6]. This constitutes a serious limitation to the broad use of PQ as an antimalarial agent. In practice, either the PQ dosage must be reduced in order to ameliorate side effects [7] or G6PD deficiency has to be tested in each patient before applying the drug [8], presenting a substantial logistical challenge in broad application of PQ. Toxicity to G6PD-deficient patients is a drawback specific to 8-aminoquinolines such as PQ and is not known to be pertinent for other quinoline drugs. In order to overcome this drawback and improve efficacy, various PQ derivatives have been synthesized and evaluated.

Recently published work bears witness that PQ derivatization and hybridization are interesting approaches in search of new antimalarials [9–22]. In particular, we have previously designed and prepared nearly a hundred primaquine derivatives of amide, urea, *bis*-urea, semicarbazide and acylsemicarbazide type, showing that they possess antiproliferative effects against human cell lines [23–29], however the antimalarial potential of these compounds has not been evaluated until now. Here we report the results of screening of selected PQ derivatives against *P.*

falciparum and a detailed QSAR study which guided the synthesis of seven new compounds of general formula **10**. They were active against malaria while exhibiting a very favorable toxicity profile towards human cells *in vitro*, which was retained even when the G6PD enzyme was inhibited.

2. Results and discussion

2.1. Chemistry

Six series of primaquine (PQ) derivatives were prepared and screened for antimalarial activity: amides **1**, ureas **2**, semicarbazides **3**, acylsemicarbazides **4**, *bis*-ureas **5** and ureidoamides **10**. Their general structures are shown in Figure 1.

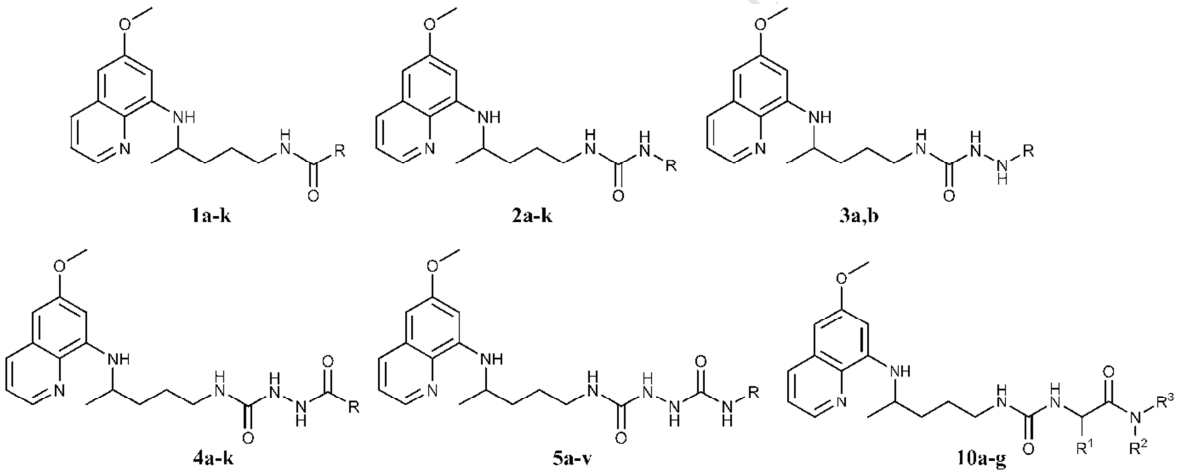

Fig. 1. Structures of the primaquine derivatives: amides **1a-k**, ureas **2a-k**, semicarbazides **3a,b**, acylsemicarbazides **4a-k**, *bis*-ureas **5a-v** and ureidoamides **10a-g**.

Syntheses of derivatives **1-5** were previously published [23–29], while ureidoamides **10** are novel compounds, described here for the first time. The synthetic pathway leading to compounds **10** is outlined in Scheme 1.

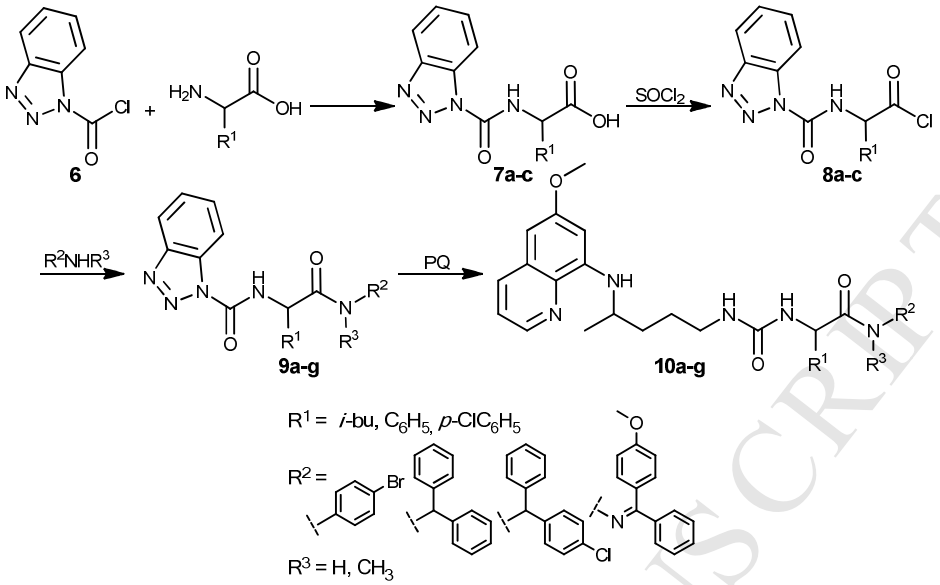

Scheme 1. Synthesis of ureidoamides **10**.

Novel ureidoamides **10a-g** with primaquine and amino acid moieties were prepared by aminolysis of *N*-(1-benzotriazolecarbonyl)-amino acid amides **9a-g** with primaquine, while amides **9** were obtained from *N*-(1-benzotriazolecarbonyl)-amino acid chlorides **8a-c** and the corresponding amines or hydrazones. Three amino acids (L-leucine, D-phenylglycine, DL-*p*-chlorophenylglycine), four amines (*p*-bromoaniline, diphenylmethanamine, (4-chlorophenyl)(phenyl)methanamine)), *N*-methyl-1,1,diphenylmethanamine and one hydrazone (4-methoxybenzophenone hydrazone) were used. Synthesis of similar ureidoamides with various amines and amino acids was previously described by our group [30,31], as well as the synthesis of the starting *N*-(1-benzotriazolecarbonyl)-amino acids **7** and their chlorides **8** [32].

The presence of the primaquine residue in compounds **10a-g** was confirmed by NMR spectra: hydrogen atoms close to pyridine nitrogen occurred in ^{1}H NMR spectra between 8.54 and 8.52, aromatic hydrogen in *p*-position from pyridine nitrogen atom at 8.09-8.06, hydrogen bound to nitrogen close to quinoline ring from 6.13 to 5.97, methoxy group at 3.82-3.81, CH of PQ chiral

carbon as a multiplet at 3.62-3.57, and finally methyl group between 1.21 and 1.19 ppm. All NH signals were D_2O exchangeable.

The presence of carbonyl groups in *N*-(1-benzotriazolecarbonyl)-amino acid amides **9a-g** was indicated by the appearance of two strong stretching vibration bands in IR spectra, the first between 1750 and 1716 cm^{-1} and the second between 1682 and 1649 cm^{-1}, while two carbonyl groups in products **10** were located at lower wavenumbers (between 1650 and 1509 cm^{-1}).

In ^{13}C NMR spectra carbonyl groups close to benzotriazole in products **9** appeared between 148.84 and 147.40 ppm and amide carbonyls between 172.20 and 167.39 ppm. Urea carbonyl groups in products **10** were shifted to lower ppm values (from 157.62 to 153.85), while amide carbonyl appeared between 172.46 and 169.45 ppm. C=N group in product **10g** appeared at 155.00 ppm. Phenyl moieties gave expected signals in aromatic region and appropriate carbon count. Structures of compounds **9f** and **9g** were confirmed indirectly, after chemical derivatization to products **10f** and **10g**, respectively.

Mass spectroscopy gave molecular ion peaks which corresponded to expected molecular formulas for all prepared compounds from series **10**. In series **9**, molecular ion peaks were visible only in spectra of **9e** and **9g**. Other compounds of general formula **9** gave only benzotriazole fragment at *m/z* 120.1 or 117.9. Chemical structures of compounds **10a-g** were also supported by CHN analyses.

2.2. Antimalarial screening

The compound series **1-5** were evaluated for their antimalarial activity against the erythrocytic stage of the *Plasmodium falciparum* NF54 strain, while an initial estimate of their cytotoxicity towards mammalian cells was obtained using the L6 cell line derived from rat skeletal

myoblasts. The IC_{50} values (the concentration of the tested compound necessary for 50% growth inhibition) and cytotoxicity data are given in Table 1. As a simple measure of a compound's potential utility, we use a selectivity index (SI), here defined as ratio of the cytotoxicity (towards L6 cells) and the antimalarial activity IC_{50} values. For reference, the SI of primaquine in our experimental system (see Materials and Methods) was 39.6.

While the majority of tested compounds exhibited a certain level of antimalarial activity, some series appeared more promising than others. For instance, all PQ-cinnamic acid derivatives of the amide type (**1a-k**) showed modest antimalarial activity, with IC_{50} roughly an order of magnitude higher than PQ, ranging between 8 and 25 µM; we note a somewhat more favorable profile in the trimethoxy derivative **1e**. Similarly, the PQ-cinnamic acid acylsemicarbazides **4a-k** showed modest activity overall, with one potential exception being the trimethoxy derivative **4e** with SI = 30 (antimalarial IC_{50} 4.5 µM and cytotoxicity 138.2 µM), thereby approximately matching the parent compound (PQ). Therefore, series **1** and **4** do not overall appear promising, with certain exceptions.

In contrast, other PQ derivative series had multiple members with favorable activity and cytotoxicity, which were dependant on the substituents. In particular, the urea series **2a-2k** contained lowly active hydroxyalkyl and cycloalkyl derivatives, however the chlorobenzhydryl urea **2i**, a compound with two PQ moieties **2k** and especially the trityl urea **2j** were active and moreover had a high SI (33, 28 and 113, respectively). Concerning the large series of *bis*-urea derivatives **5a-v**, hydroxyalkyl and cycloalkyl derivatives were again lowly active. Halogenated aryl and biaryl derivatives had modest activity (IC_{50} from 7.5 to 17.8 µM) and exhibited some cytotoxicity. The most interesting compound was again the trityl derivative **5r**, which exhibited SI > 80 (IC_{50} 1.2 µM and cytotoxicity >100 µM). Furthermore, compound **5v** bearing a

dimethoxybenzhydryl substituent was highly active (at PQ-like levels, 2.2 µM). The two semicarbazides in series **3** (**3a** and **3b**), which also bear methoxybenzhydryl groups, showed high activity and low cytotoxicity as well.

In summary, the trityl compounds **2j** and **5r** represent active PQ derivatives with apparently improved selectivity over the parent compound, PQ (SI 113 and 80, respectively, compared to SI of primaquine 39.6), as estimated in our experimental system. The dimethoxybenzhydryl compounds **3b** and **5v** also appear highly promising, with SI 78.3 and 61.8, respectively. Motivated by these examples where favorable biological properties appear linked to certain substituents, we further developed a QSAR model to direct the synthesis of a novel series of antimalarial lead compounds based on PQ.

Table 1

In vitro screening of primaquine derivatives against erythrocytic stage of *P. falciparum* and cytotoxicity towards L6 rat cells.

Compd.	Structural formula	Antimalarial activity [a] IC_{50}, µM	Cytotox-icity [a] IC_{50}, µM	SI [b]	Synth. Ref. [c]	QSAR train/test set
1a	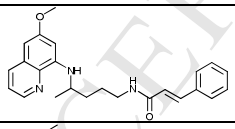	15.1	18.5	1.2	[29]	Test
1b	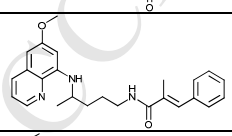	>24.8	>250	10.1	[29]	Test
1c	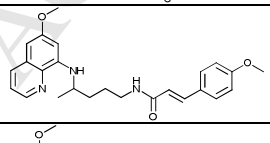	12.4	>240	19.4	[29]	Test
1d	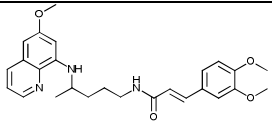	11.9	>220	18.5	[29]	Test

1e	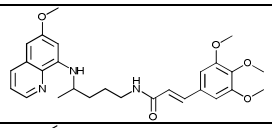	8.1	>210	25.9	[29]	Test
1f	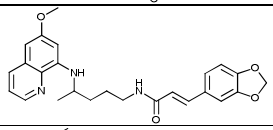	22.1	29	1.3	[29]	Test
1g	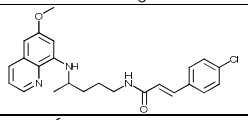	13.7	16.8	1.2	[29]	Test
1h	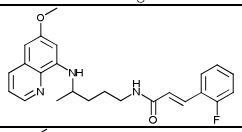	13.2	3.5	0.3	[29]	Test
1i	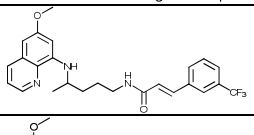	15.6	16.2	1.0	[29]	Test
1j	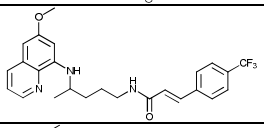	12.9	160	12.4	[29]	Test
1k	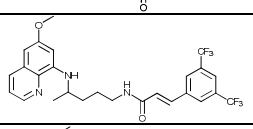	11.3	158.1	14.0	[29]	Test
2a	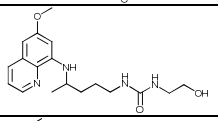	27.4	n.d.[d]	n.d.	[24]	Train
2b	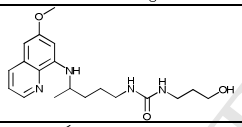	52.4	n.d.	n.d.	[24]	Train
2c	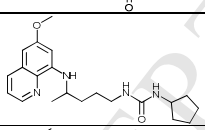	65.9	n.d.	n.d.	[23]	Train
2d	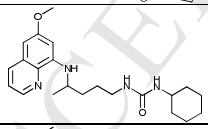	42.1	n.d.	n.d.	[23]	Train
2e	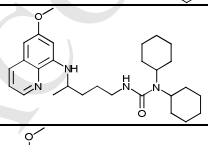	8.1	n.d.	n.d.	[23]	Train
2f	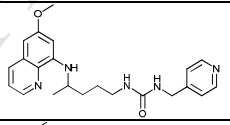	47.3	n.d.	n.d.	[23]	Train
2g	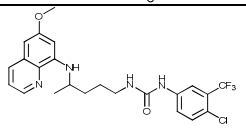	17.1	n.d.	n.d.	[26]	Train

2h	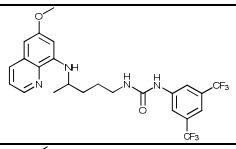	11.9	14.9	1.3	[28]	Test
2i	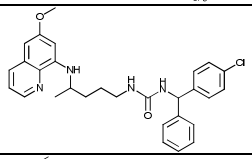	4.3	140	32.6	[26,27]	–
2j	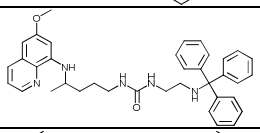	1.5	>171	114.0	[26]	Train
2k	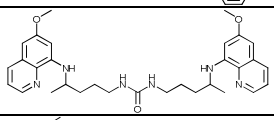	6.4	>180	28.1	[26]	Train
3a	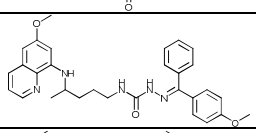	4.1	>195	47.6	[26]	Train
3b	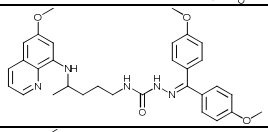	2.3	>180	78.3	[26]	Train
4a	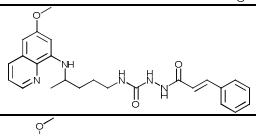	17.2	13.9	0.8	[29]	Test
4b	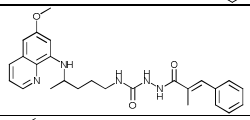	22.9	36.5	1.6	[29]	Test
4c	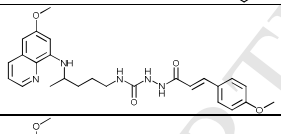	22.2	3.6	0.2	[29]	Test
4d	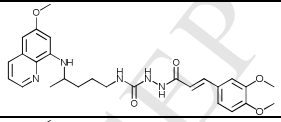	>19.7	37	1.9	[29]	Test
4e	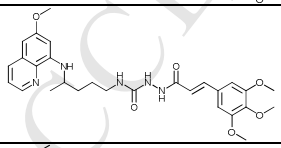	4.5	138.2	30.7	[29]	Test
4f	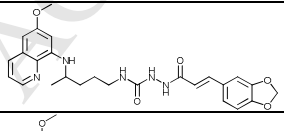	20.4	15.5	0.8	[29]	Test
4g	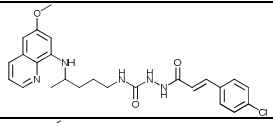	24.2	7.3	0.3	[29]	Test
4h	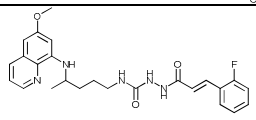	>21.4	25.1	1.2	[29]	Test

4i	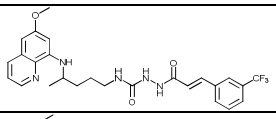	>19.4	10.6	0.5	[29]	Test
4j	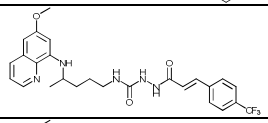	>19.4	28.3	1.5	[29]	Test
4k	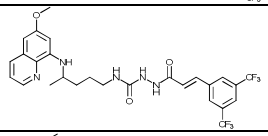	>17.1	>170	9.9	[29]	Test
5a	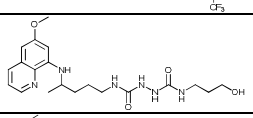	58.8	n.d.	n.d.	[26]	Train
5b	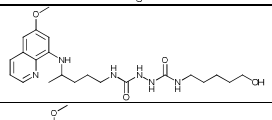	43.7	n.d.	n.d.	[26]	Train
5c	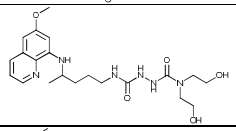	41.4	178.1	4.3	[26,27]	–
5d	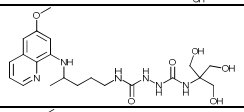	66.7	n.d.	n.d.	[26]	Train
5e	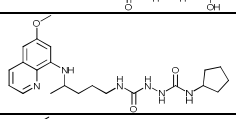	75.4	n.d.	n.d.	[25]	Train
5f	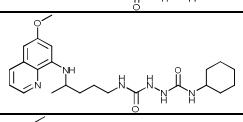	46.3	n.d.	n.d.	[25]	Train
5g	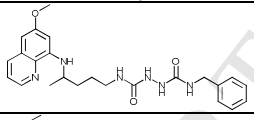	>111.0	n.d.	n.d.	[25]	Train
5h	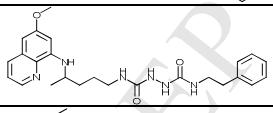	27.1	n.d.	n.d.	[25]	Train
5i	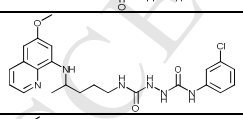	14.9	58.6	3.9	[28]	Test
5j	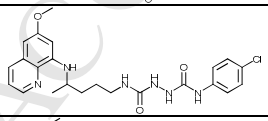	17.8	91.9	5.2	[28]	Test
5k	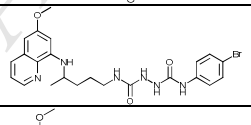	17.8	38.7	2.2	[28]	Test
5l	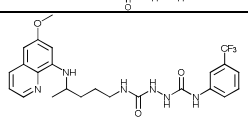	11.8	32.1	2.7	[28]	Test

5m	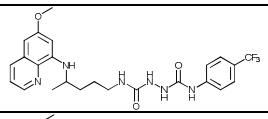	10.3	14.9	1.4	[28]	Test
5n	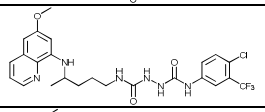	15.2	n.d.	n.d.	[26]	Train
5o	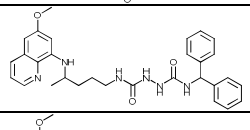	10.3	n.d.	n.d.	[25]	Train
5p	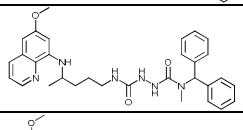	10.0	10.4	1.0	[26]	Test
5q	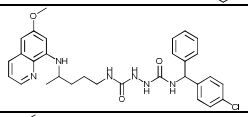	7.5	8.4	1.1	[26,27]	–
5r	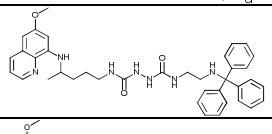	1.2	>100	83.3	[26]	Test
5s	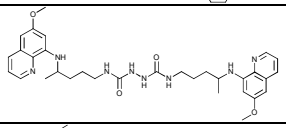	3.7	76.6	20.7	[26,27]	–
5t	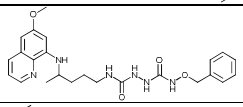	20.8	n.d.	n.d.	[25]	Train
5u	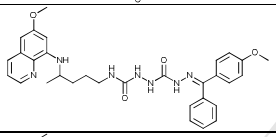	5.6	16.0	2.9	[26]	Train
5v	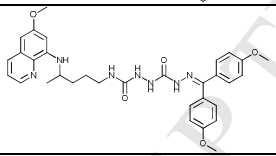	2.2	136.1	61.9	[26]	Train
10a	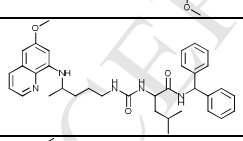	3.4	>170	50.0	this work	Test
10b	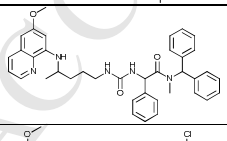	6.5	>140	21.5	this work	Test
10c	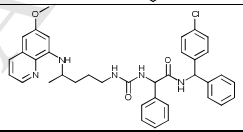	3.0	>160	53.3	this work	Test
10d	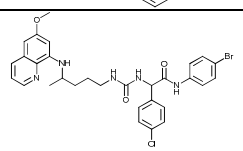	3.2	54.0	16.9	this work	Test

10e	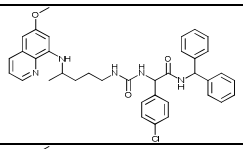	1.4	>160	114.3	this work	Test
10f	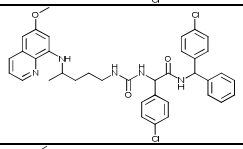	1.8	>150	83.3	this work	Test
10g	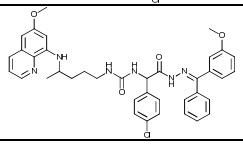	2.7	>120	44.4	this work	Test
PQ diphosphate		1.5	59.5	39.7		

[a] IC_{50} – the concentration of the compound necessary for 50% growth inhibition of *P. falciparum* or L6 rat myoblast cells; the displayed numbers are averages of two or three independent experiments. [b] SI - selectivity index, defined as a ratio of the cytotoxicity and the antimalarial activity. [c] Reference for synthesis. [d] n.d. – not determined.

2.3. Quantitative structure-activity relationship modeling

The QSAR model for prediction of antimalarial activity (log IC_{50} against the *P. falciparum* NF54 strain) was trained using the Support Vector Machines (SVM) algorithm. SVMs are a machine learning method known to have a high predictive accuracy and to generalize well to novel data sets and are therefore increasingly used also for QSAR studies [33], including our previous work for modeling biological activity of peptides, ionophores, and substrate specificity of a human protein [34–36]. Here, the SVM regression model was trained on a set of 56 compounds (structures provided in Supporting Information), which consisted of 23 PQ derivatives from this study (series **1**-**5**; Table 1) and additional 33 compounds from published data by Kaur *et al*. [37–39] that were sufficiently similar in structure to the original 23 compounds; see Materials and Methods for how the QSAR applicability domain was defined. The SVM model had a high accuracy in predicting activity against *P. falciparum* when tested in cross-validation: $R^2 = 0.776$; root-mean-square error (RMSE) = 0.294 when predicting $\log_{10}$ IC_{50} units (Figure 2a). In other

words, we estimate that our SVM model can predict the IC_{50} of a PQ derivative within a 1.97-fold range of the actual value ($10^{0.294}$). Moreover, the model retained much of the predictive accuracy when tested on an independent test set of 37 PQ derivatives that are within the model's applicability domain (see Materials and Methods), yielding a RMSE = 0.403 $\log_{10}$ units of IC_{50} (Figure 2b), implying a good qualitative agreement of the model to observed data. If the compounds are classed into two groups, lowly active (above-median $IC_{50} \geq 8.9$ μM) and highly active (below-median $IC_{50} < 8.9$ μM) compounds, our predictions would be 91% accurate on the training set, and 95% accurate on the independent test set (measuring the fraction compounds assigned to the correct class; Figure 2d). Therefore, this appears to be a useful statistical model to prioritize the synthesis of further PQ derivatives with antiplasmodial activity.

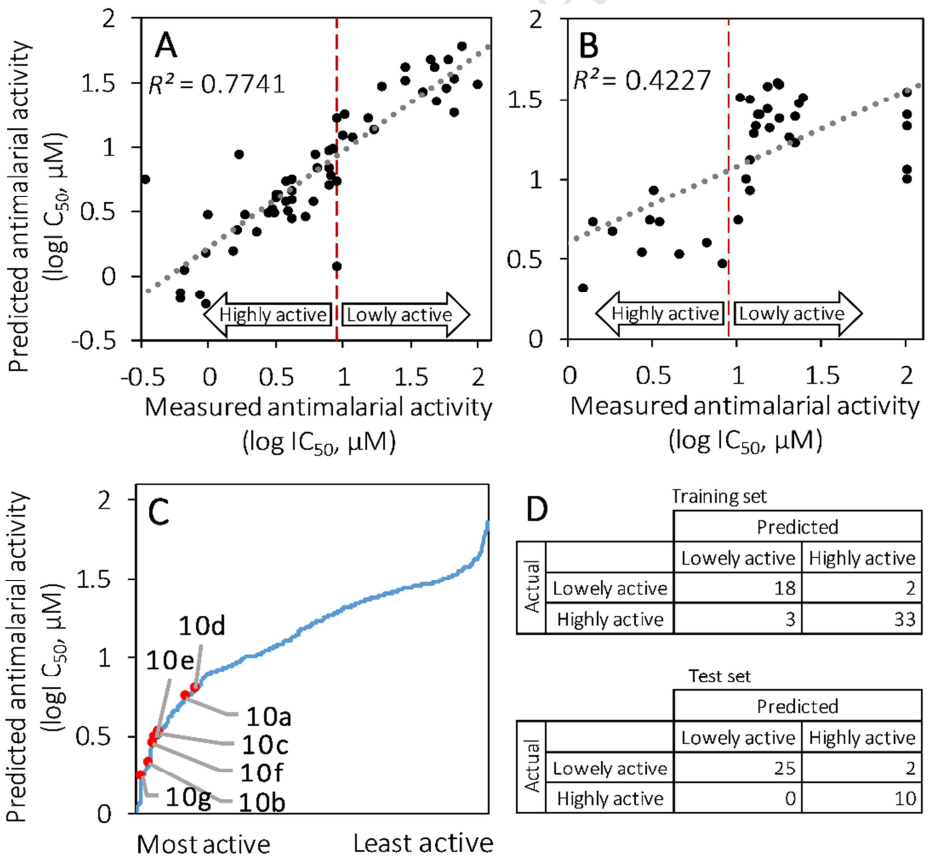

Fig. 2. Measured and predicted activity of 56 training set compounds (A) and 37 testing compounds (B); Predicted activities of an in house library of 522 compounds, sorted from the most active to the least active compound (C); Qualitative agreements of the model's predictions with the observed data (D). Novel ureidoamides **10a-g** are marked with red dots. Predicted activities for the training compounds were obtained in ten-fold cross-validation.

Next, the SVM model was applied to infer the antimalarial activity of an in-house virtual library of 522 molecules; the structures and activity predictions are supplied in Supporting Information. Based on their high predicted antimalarial activity (Figure 2c) and further considerations related to chemical synthesis, seven PQ ureidoamides **10a-g** bearing an amino acid residue were selected for synthesis and evaluation against *P. falciparum* and for an initial cytotoxicity screen using the L6 mammalian cell line.

2.4. Antimalarial activity and cytotoxicity of novel PQ ureidoamides

Indeed, four out of seven compounds from the series **10** showed a favorable cytotoxicity/antimalarial activity ratio, with SI > 50 (PQ has SI = 39.6). The benzhydryl ureidoamide derived from *p*-chlorophenylglycine **10e** was the most promising of all 64 tested compounds, with SI > 114, followed by chlorobenzhydryl derivative **10f** with SI > 83. While the compounds **10e** and **10f** have very similar antiplasmodial activity as the parent compound, PQ (Table 1), they are at least 2.7 and 2.5-fold less cytotoxic relative to PQ in this particular *in vitro* model using L6 rat skeletal myoblasts. Of note, these are conservative estimates, given that the L6 experimental assay reached the boundary of its detection range; in other words, the actual toxicity of **10e** and **10f** may be even lower.

To follow up on the initial observation of reduced cytotoxicity in rat L6 cells, we performed growth inhibition screens on four human tumor cell lines from diverse tissues: H460 (lung), MCF-7 (breast), SW620 (colon) and A2780 (ovary); Table 2. For the novel compounds in series **10**, human cell lines suggest at least an order of magnitude reduced cytotoxicity compared to PQ (Tables 2 and S1). Compound **10e** in particular did not reach IC_{50} up to the maximum tested concentration of 100 μM in three of the four cell lines, and similarly so for **10f**. Therefore, **10e** and **10f** are at least 13-fold less toxic than PQ, which has median IC_{50} across cell lines 7.5 μM (range 5 to 14 μM) in this model system (Table 2). Compound **10c** also exhibits a favorable toxicity profile (non-toxic up to 100 μM in all four human cell lines; Table 2) and retains much of the activity (*P. falciparum* IC_{50} = 3.0 μM). In this respect, the novel compounds **10** appear to be a large improvement over other PQ derivative series tested here: while the above-reported compounds **3b**, **5r** and **5v** exhibited PQ-like antimalarial activity (Table 1), they are also similarly cytotoxic to human cells as PQ (Table 2), in stark contrast to **10c**, **10e** and **10f** which are substantially less cytotoxic than PQ. Of note, our data for **10c**, **10e** and **10f** were measured across five independent experiments (biological replicates) for the H460 and MCF-7 cell lines and at least two experiments in SW620 and A2780 cells (Table 2), suggesting robust results. To further examine effects on a broader panel of human tissues, we also tested against the tumor-derived cell lines HCT 116 (colon), HL-60 and K562 (blood/myeloid lineage) and Capan-1 (pancreatic). All compounds from series **10** had very low cytotoxicity also on all these additional cell lines (IC_{50} >100 μM; single biological replicate), unlike PQ (Table S1).

Table 2

IC_{50} values[a] (in μM; mean ± standard deviation) for human cell lines

Compd.	Cell lines			
	H460	MCF-7	SW620	A2780
3b	> 100 (n = 3)[b]	3 ± 0.4 (n = 2)	>100[c] (n = 2)	1 ± 0.1 (n = 3)
5r	3 ± 0.3 (n = 2)	3 ± 2 (n = 2)	7 ± 4[c] (n = 2)	1 ± 0.2 (n = 2)
5v	5 ± 0.3 (n = 2)	1 ± 0.5 (n = 2)	> 100[c] (n = 2)	0.06 ± 0.01 (n = 3)
10a	> 100 (n = 5)	> 100 (n = 4)	>100 (n = 3)	36±29 (n = 3)
10b	64 ± 32 (n = 2)	> 100 (n = 2)	>100 (n = 3)	n. t.[d]
10c	> 100 (n = 5)	> 100 (n = 5)	>100 (n = 3)	> 100 (n = 2)
10d	52 ± 31 (n = 2)	16 ± 0.2 (n = 2)	32 ± 8 (n = 3)	n. t.
10e	> 100 (n = 5)	> 100 (n = 5)	6 ± 1 (n = 3)	> 100 (n = 2)
10f	> 100 (n = 5)	> 100 (n = 5)	> 100 (n = 3)	14 ± 4 (n = 2)
10g	> 100 (n = 2)	> 100 (n = 2)	> 100 (n = 3)	n. t.
PQ	10 ± 5 (n = 3)	5 ± 2 (n = 6)	14 ± 2 (n = 3)	5 ± 0.2 (n = 2)

[a] IC_{50} – the concentration that causes 50% growth inhibition. [b] Number of independent experiments (biological replicates) given in parentheses. [c] Values previously reported by Pavić *et al.* [23]. [d] n. t. – not tested.

2.5. Cytotoxicity in G6PD-deficient cells

One important mechanism of PQ toxicity in patients is related to the G6PD enzyme, wherein the persons with an inherited deficiency of G6PD may suffer severe side effects, in particular hemolytic anemia [40,41]. We therefore asked whether the favorable cytotoxicity profile of novel compounds **10** is retained or abolished in G6PD-deficient cells, in comparison to PQ and the most promising previous PQ derivatives from series **3** and **5**. To investigate, we applied a

G6PD inhibitor 6-aminonicotinamide (6-AN) to the human cell lines H460 and MCF-7, thereby reducing G6PD activity in the cells. We observed that in highly active PQ derivatives **3b**, **5r** and **5v**, the cytotoxicity is aggravated upon G6PD inhibition (Figures 3c and 3d), similarly as for PQ itself (Figures 3a and 3b).

In particular, applying 10 µM of PQ by itself lowers the MCF-7 cell growth rate to 25% of the untreated cells (meaning, growth is reduced by three-quarters, but there is still a net increase in number of cells; Figures 3a and 3b). However, the same PQ concentration in combination with 6-AN (at 10 µM) results in a negative growth rate of approx. –45%, meaning there is much cell death occurring caused by PQ in the G6PD-inhibited cells. In other words, there is a synergistic effect on cytotoxicity by PQ and G6PD inhibition (Figures 3a and 3b). In contrast, a highly cytotoxic cancer drug not known to act in a G6PD-dependent manner, paclitaxel, does not show synergies with 6-AN (Figures 3a and 3b). The toxicity of 6-AN itself – always applied at 10 µM – for the H460 and MCF-7 cell lines is modest and thus unlikely to confound results (82% growth rate for MCF-7 and 87% for H460 for 6-AN only).

We next turned to examine the effects of G6PD inhibition on the cytotoxicity of the novel compounds **10a**, **10c**, **10e** and **10f** in human cell lines (Figures 3e and 3f). There was little difference in growth inhibition of the H460 and MCF-7 cells regardless of if the G6PD inhibitor was simultaneously applied or not. In particular, at 10 µM, compound **10e** results in >50% MCF-7 cell growth with or without 6-AN (80% vs. 65%) and equally so with the compound **10f** (93% vs. 76%). The observable difference is in line with the effect size due to applying 6-AN itself (approx. 15%) and therefore there does not appear to be a synergistic effect of **10e** and **10f** with G6PD inhibition, unlike PQ (25% *vs*. –45%, which amounts to a 70% difference) and unlike the previous compounds **3b**, **5r** and **5v** (Figure 3c and 3d). The compounds **10a** and **10c** show a

similar pattern, indicating that G6PD inhibition does not substantially aggravate their toxicity (Figures 3e and 3f). H460 cells broadly uphold these results for **10a**, **10c** and **10f**. Overall, our data suggest that the novel PQ derivatives synthetized herein are promising lead compounds for antimalarial drugs with an improved safety profile for G6PD-deficient patients. Testing of compounds **10** and their derivatives in other cell types and in model animals is therefore warranted to further establish the medicinal potential of these novel PQ derivatives.

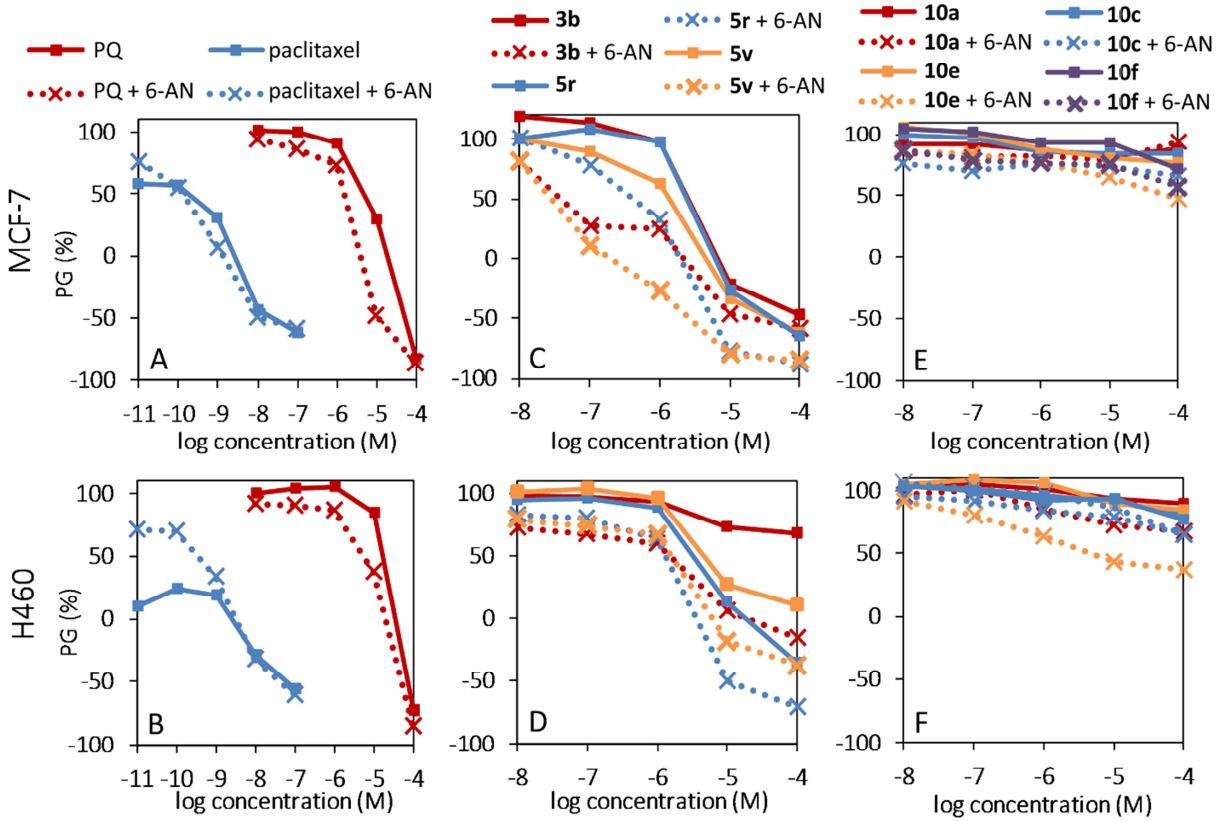

Fig. 3. The effects of G6PD inhibition on the cytotoxicity of the compounds to MCF-7 and H460 cell lines; controls (A and B), PQ-derivatives (C and D) and newly synthetized ureidoamides (E and F).

2.6. A comprehensive resource of predicted antimalarial activity and cytotoxicity of PQ-like compounds

Our efforts to computationally model the structure-activity relationship of PQ derivatives resulted in a highly accurate predictor based on the SVM algoritm. We were thus further motivated to employ computational modeling to provide a library of predictions for a broad set of 13,401 PQ-like molecular structures extracted from PubChem; see Supporting Text S1 for a description of the modeling, and see Supporting Information for the inferred biological activities. In brief, we predicted 199 compounds to be simultaneously more active and less cytotoxic than PQ itself (predictions listed in Supporting Information). While we took precautions to ensure that the molecular structures of the >13,000 tested compounds are reasonably consistent with the training set of PQ derivatives (see section 4.3.3), we advise caution in interpreting the predictions, given that QSAR models tend to become less reliable as structures diverge. We recovered individual examples of correct predictions in this data set, as suggested by a literature search (see Supporting Text S1 and Figure S1). If further validated by independent data, this database of predicted activities could serve as a useful resource to inspire future research on antimalarial PQ derivatives.

3. Conclusions

PQ and its derivatives are important drugs for treatment of various types of malaria, where in particular PQ has a unique ability to prevent *P. falciparum* transmission by killing the gametocytes of the parasite in the bloodstream. However, applying PQ at a broad scale is complicated by severe toxicity towards a subset of patients with an inherited G6PD deficiency. Therefore, there is a need for novel derivatives of PQ which would retain or improve its efficacy, while presenting a more favorable toxicity profile. Here, we evaluated the activity of 64 diverse PQ derivatives against the erythrocytic stage of the *P. falciparum* NF54 strain. PQ-cinnamic acid amides **1d** and **1e**, chlorobenzhydryl **2i**, trityl **2j** and **2k** urea with two PQ residues, PQ-cinnamic

acid semicarbazide **4e**, the trityl *bis*-urea **5r** and the methoxybenzhydryl compounds **3b** and **5v** showed high activities. Based on these experimental measurements, a QSAR model prioritized a novel series of PQ ureidoamides **10a-g** that we designed, prepared and evaluated against *P. falciparum* and mammalian cells. The results confirmed high activity and low cytotoxicity of ureidoamides **10**, especially of benzhydryl and chlorobenzhydryl compounds **10e** and **10f** derived from *p*-chlorophenylglycine. These showed antimalarial activity comparable with PQ, but at least an order of magnitude lower cytotoxicity to various human cell types and in particular their toxic effects were not notably aggravated in G6PD-inhibited cells, in contrast to PQ. We suggest that **10a-g** constitute promising lead compounds for development of more effective and safer drugs for malaria treatment, particularly for G6PD-deficient patients. Furthermore, our computational models predict hundreds of additional PQ-related compounds with favorable antimalarial activity and cytotoxicity profiles, highlighting new avenues for future research efforts.

4. Materials and methods

4.1. Synthesis

4.1.1. General information

Melting points were measured on a Stuart Melting Point (SMP3) apparatus (Barloworld Scientific, UK) in open capillaries with uncorrected values. IR spectra were recorded on FTIR Perkin Elmer Spectrum One and UV-Vis spectra on Lambda 20 double beam spectrophotometer (Perkin-Elmer, UK). All NMR (^{1}H and ^{13}C) were recorded at 25 °C on NMR Avance 600 spectrometer (Bruker, Germany) at 300 and 150 MHz for ^{1}H and ^{13}C nuclei, respectively.

Chemical shifts (δ) are reported in parts per million (ppm) using tetramethylsilane as reference in the ^{1}H and the DMSO residual peak as reference in the ^{13}C spectra (39.51 ppm). Coupling constants (J) are reported in Hertz (Hz). Mass spectra were recorded on HPLC-MS/MS (HPLC, Agilent Technologies 1200 Series; MS, Agilent Technologies 6410 Triple Quad). Mass determination was realized using electron spray ionization (ESI) in positive or negative mode. CEM Discover microwave reactor was used for microwave reactions (P = 150 W, t = 70 °C). Elemental analyses were performed on a CHNS LECO analyzer (LECO Corporation, USA). Found values for carbon, hydrogen and nitrogen were within ± 0.4% of the theoretical values. All compounds were routinely checked by TLC with Merck silica gel 60F-254 glass plates using the following solvent systems: petrolether/ethyl acetate/methanol 30:10:5, cyclohexane/ethyl acetate 1:1, cyclohexane/ dichloromethane/methanol 10:18:2, dichloromethane/dichloromethane/methanol 97:3 and 95:5. Spots were visualized by short-wave UV light and iodine vapour. Column chromatography was performed on silica gel 0.063–0.200 mm (Kemika, Croatia) and 0.040–0.063 mm (Merck, Germany), with the same eluents used in TLC.

1*H*-benzo[*d*][1,2,3]triazole (BtH), triphosgene, triethylamine (TEA), hydrazine hydrate, L-leucine, D-phenylglycine, DL-*p*-chlorophenylglycine, *p*-bromoaniline and *N*-methyl-1,1-diphenylmethanamine were purchased from Sigma-Aldrich. Primaquine, diphenylmethanamine and (4-chlorophenyl)(phenyl)methanamine were prepared from commercially available salts (Sigma-Aldrich) prior the use. All reactions with primaquine were run light protected. 1-Benzotriazole carboxylic acid chloride (BtcCl, **6**) was prepared according to our procedures published earlier [42,43]. 4-Methoxybenzophenone hydrazone was prepared from 4-

methoxybenzophenone and hydrazine hydrate [44]. Primaquine derivatives **1-5** were prepared according to the previously published procedures [23–29].

*4.1.2. Btc-amino acids (7a-**c**): general procedure*

To a suspension of 20 mmol of amino acid in dry dioxane (40 ml) a solution of 1.81 g (10 mmol) BtcCl (**6**) in dry dioxane (10 ml) was added dropwise. The reaction mixture was stirred overnight at room temperature. Amino acid hydrochloride was filtered off, washed with dioxane and the mother liquor was evaporated under reduced pressure. The crude products were triturated several times with hot toluene. 2-[(1*H*-1,2,3-benzotriazole-1-carbonyl)amino]-4-methylpentanoic acid (Btc-L-leucine, **7a**) and 2-[(1*H*-1,2,3-benzotriazole-1-carbonyl)amino]-2-phenylacetic acid (Btc-D-phenylglycine, **7b**) were described in our previous paper [32], while 2-[(1*H*-1,2,3-benzotriazole-1-carbonyl)amino]-2-(4-chlorophenyl)acetic acid (Btc-DL-*p*-chlorophenylglycine, **7c**) is a new compound.

*4.1.2.1. 2-[(1H-1,2,3-benzotriazole-1-carbonyl)amino]-2-(4-chlorophenyl)acetic acid (Btc-DL-p-chlorophenylglycine (**7c**)*

From the reaction of 3.712 g *p*-chlorophenylglycine and 1.81 g chloride **6**, 3.274 g (99%) of **7c** was obtained; mp 127 ^{o}C (decomp.); IR (KBr): ν_{max} 3360, 2924, 2540, 1750, 1712, 1494, 1450, 1380, 1290, 1184, 1136, 1064, 1018, 976, 932, 822, 786, 754, 732, 680, 662, 642, 624, 600, 558, 538, 516, 466 cm^{-1}; ^{1}H NMR (DMSO-d_6) δ 9.63-9.62 (d, J = 7.21 Hz, 1H), 8.24-8.22 (d, J = 8.35 Hz, 1H), 8.16-8.14 (d, J = 8.30 Hz, 1H), 7.75-7.71 (t, J = 7.56 Hz, 1H), 7.63-7.61 (d, J = 8.46 Hz, 2H), 7.59-7.55 (t, J = 7.72 Hz, 1H), 7.49-7.47 (d, J = 8.45 Hz, 2H), 7.18-7.17 (d, J = 7.24 Hz, 1H), 5.71-5.69 (d, J = 7.20 Hz, 1H); ^{13}C NMR (DMSO-d_6) δ 170.66, 148.50, 145.48, 135.76, 132.81, 131.25, 130.22, 130.14, 128.41, 125.76, 119.94, 113.38, 56.69; ESI-MS; *m/z*

calculated for $C_{15}H_{11}ClN_4O_3$: 330.05, found: 353.2 $(M+23)^+$; calculated for $C_6H_9N_3$: 119.12, found: 120.1 $(BtH+1)^+$.

*4.1.3. Btc-amino acid chlorides (**8a-c**): general procedure*

A solution of 4 mmol Btc-amino acid in 20 ml thionyl chloride was stirred overnight at room temperature. Thionyl chloride was evaporated under reduced pressure and the residue was dissolved in dry toluene and evaporated again (several times). Crude products **8a-c** were used immediately in further reactions.

*4.1.4. Btc-amino acid amides (**9a-g**): general procedure*

A solution of 3.4 mmol corresponding amine or hydrazone and 4 mmol TEA in dry toluene (20 ml) was added dropwise to a solution of 4 mmol chloride **8** in dry toluene (30 ml). The reaction mixture was stirred 30 min at room temperature. TEA × HCl was filtered off and mother liquor was evaporated. The residue was dissolved in ethyl acetate/1% HCl mixture (1:1). The organic layer was extracted three times with HCl solution (w = 1%), washed two times with water, dried over anhydrous sodium sulfate, filtered and evaporated under reduced pressure.

*4.1.4.1. 2-[(1H-1,2,3-benzotriazole-1-carbonyl)amino]-N-(diphenylmethyl)-4-methylpentanamide (**9a**)*

From the reaction of 0.623 g diphenylmethanamine, 1.179 g chloride **8a** and 0.404 g TEA, and after trituration with ether, 1.081 g (72%) of **9a** was obtained; mp 155–158 °C; IR (KBr): ν_{max} 3328, 3261, 3068, 2958, 2929, 1716, 1650, 1557, 1522, 1450, 1378, 1287, 1230, 1152, 1079, 1050, 1013, 925, 855, 836, 753, 699, 633, 567, 521, 462 cm^{-1}; ^1H NMR (DMSO-d_6) δ 9.12-9.09 (2d, J = 3.95 Hz, 2H'), 8.23-8.18 (m, 2H), 7.76-7.72 (t, J = 7.71 Hz, 1H), 7.58-7.55 (t, J = 7.68

Hz, 1H), 7.37-7.24 (m, 10H), 6.18-6.16 (d, *J* = 8.37 Hz, 1H), 4.71-4.65 (m, 1H), 1.94-1.88 (m, 1H), 1.73-1.62 (m, 2H), 0.95-0.89 (d, *J* = 6.48 Hz, 6H); ^{13}C NMR (DMSO-d_6) δ 170.58, 148.84, 145.47, 142.19, 142.08, 131.32, 130.06, 128.40, 128.34, 127.49, 127.24, 127.05, 125.65, 119.84, 113.54, 56.08, 52.97, 38.89, 24.46, 23.08, 21.38 [45].

*4.1.4.2. 2-[(1H-1,2,3-benzotriazole-1-carbonyl)amino]-N-(diphenylmethyl)-N-methyl-2-phenylacetamide (**9b**)*

From the reaction of 0.671 g *N*-methyl-1,1-diphenylmethanamine, 1.259 g chloride **8b** and 0.404 g TEA, and after purification by column chromatography (mobile phase cyclohexane/ethyl acetate/methanol 30:10:5), 0.857 g (53%) of **9b** was obtained; mp 82–83.5 ^{o}C; IR (KBr): ν_{max} 3377, 3032, 2939, 1735, 1649, 1490, 1405, 1294, 1231, 1081, 1033, 932, 867, 813, 753, 702, 611, 569, 519 cm^{-1}; ^{1}H NMR (DMSO-d_6) δ 9.16-9.14 (d, *J* = 5.97 Hz, 1H), 8.22-8.14 (m, 2H), 7.75-7.70 (t, *J* = 8.27 Hz, 1H), 7.54 (m, 3H), 7.43-7.21 (m, 11H), 7.02-6.93 (m, 2H), 6.53 (s, 1H), 6.16-6.14 (d, *J* = 6.23 Hz, 1H), 2.67 (s, 3H); ^{13}C NMR (DMSO-d_6) δ 169.24, 147.40, 145.50, 138.47, 138.24, 135.92, 131.08, 130.26, 128.80, 128.60, 128.51, 128.48, 128.42, 128.28, 127.51, 125.71, 119.97, 113.28, 61.00, 55.58, 31.69.

*4.1.4.3. 2-[(1H-1,2,3-benzotriazole-1-carbonyl)amino]-N-[(4-chlorophenyl)(phenyl)methyl]-2-phenylacetamide (**9c**)*

From the reaction of 0.740 g (4-chlorophenyl)(phenyl)methanamine, 1.259 g chloride **8b** and 0.404 g TEA, and after trituration with ether/petroleum ether and purification of mother liquid by column chromatography (mobile phase cyclohexane/ethyl acetate/methanol 30:10:5), 1.400 g (83%) of **9c** was obtained; mp 116–118.5 ^{o}C; IR (KBr): ν_{max} 3286, 3062, 3032, 1748, 1660, 1502, 1499, 1448, 1380, 1232, 1182, 1126, 1094, 1036, 934, 852, 812, 752, 698, 612, 572, 554, 518, 496 cm^{-1}; ^{1}H NMR (DMSO-d_6) δ 9.41-9.39 (t, *J* = 7.41 Hz, 1H), 9.03-9.01 (d, *J* = 7.14 Hz,

1H), 8.23-8.21 (d, *J* = 8.29 Hz, 1H), 8.15-8.13 (dd, *J* = 2.6 Hz, 8.3 Hz, 1H), 7.74-7.71 (t, *J* = 7.60 Hz, 1H), 7.61-7.60 (d, *J* = 7.81 Hz, 2H), 7.87-7.55 (t, *J* = 7.91 Hz, 1H), 7.43-7.35 (m, 6H), 7.32-7.28 (m, 2H), 7.25-7.21 (m, 2H), 7.11-7.08 (t, *J* = 7.37 Hz, 2H), 6.19-6.17 (d, *J* = 8.10 Hz, 1H), 5.84-5.81 (t, *J* = 6.46 Hz, 1H); ^{13}C NMR (DMSO-d_6) δ 172.20, 148.06, 145.50, 141.21, 140.76, 135.60, 132.20, 131.15, 130.21, 129.40, 128.79, 128.51, 128.26, 128.19, 128.05, 128.00, 126.72, 125.69, 119.91, 113.33, 59.56, 56.54.

*4.1.4.4. 2-[(1H-1,2,3-benzotriazole-1-carbonyl)amino]-N-(4-bromophenyl)-2-(4-chlorophenyl)acetamide (**9d**)*

From the reaction of 0.585 g *p*-bromoaniline, 1.397 g chloride **8c** and 0.404 g TEA, and after purification by column chromatography (mobile phase cyclohexane/ethyl acetate/methanol 30:10:5) and trituration with ether/petroleum ether and toluene/petroleum ether, 0.989 g (60%) of **9d** was obtained; 168.5–169.5 ^{o}C; IR (KBr): ν_{max} 3406, 3232, 3062, 1732, 1656, 1600, 1498, 1452, 1396, 1346, 1290, 1218, 1092, 1014, 930, 818, 778, 754, 724 ,656, 628, 594, 540, 502 cm^{-1}; ^{1}H NMR (DMSO-d_6) δ 10.63 (s, 1H), 9.48-9.47 (d, *J* = 7.14 Hz, 1H), 8.24-8.22 (d, *J* = 8.31 Hz, 1H), 8.16-8.14 (d, *J* = 8.33 Hz, 1H), 7.75-7.71 (t, *J* = 7.55 Hz, 1H), 7.67-7.65 (d, *J* = 8.50 Hz, 2H), 7.60-7.57 (t, *J* = 7.38 Hz, 3H), 7.55-7.48 (m, 4H), 5.83-5.82 (d, *J* = 7.18 Hz, 1H); ^{13}C NMR (DMSO-d_6) δ 167.39, 148.52, 145.48, 137.78, 135.92, 133.04, 131.72, 131.24, 130.22, 129.80, 128.62, 125.77, 121.47, 119.95, 115.62, 113.39, 57.58.

*4.1.4.5. 2-[(1H-1,2,3-benzotriazole-1-carbonyl)amino]-2-(4-chlorophenyl)-N-(diphenylmethyl)acetamide (**9e**)*

From the reaction of 0.623 g diphenylmethanamine, 1.397 g chloride **8c** and 0.404 g TEA, and after trituration several times with ether/petroleum ether, 0.640 g (38%) of **9e** was obtained; mp 164.5–166.5 ^{o}C; IR (KBr): ν_{max} 3388, 3276, 3062, 1732, 1682, 1648, 1492, 1448, 1380, 1288,

1218, 1094, 1024, 930, 818, 750, 702, 648, 590, 566, 540 cm^{-1}; ^{1}H NMR (DMSO-d_6) δ 9.41-9.40 (d, J = 8.23 Hz, 1H), 9.10-9.09 (d, J = 7.29 Hz, 1H'), 8.23-8.21 (d, J = 8.36 Hz, 1H), 8.14-8.12 (d, J = 8.31 Hz, 1H), 7.74-7.71 (t, J = 7.85 Hz, 1H), 7.64-7.62 (d, J = 8.52 Hz, 2H), 7.57-7.54 (t, J = 8.59 Hz, 1H), 7.47-7.46 (d, J = 8.04 Hz, 2H), 7.37-7.35 (m, 2H), 7.32-7.31 (d, J = 7.07 Hz, 2H), 7.29-7.28 (m, 1H), 7.27-7.20 (m, 3H), 7.10-7.08 (d, J = 7.01 Hz, 2H), 6.17-6.15 (d, J = 8.20 Hz, 1H), 5.84-5.83 (d, J = 7.23 Hz, 1H); ^{13}C NMR (DMSO-d_6) δ 167.71, 148.10, 145.47, 141.62, 141.60, 136.63, 132.79, 131.15, 130.18, 129.27, 128.44, 128.42, 128.29, 127.55, 127.22, 127.04, 126.85, 125.69, 119.90, 113.31, 56.55, 56.34.

*4.1.4.6. 2-[(1H-1,2,3-benzotriazole-1-carbonyl)amino]-2-(4-chlorophenyl)-N-[(4-chlorophenyl)(phenyl)methyl]acetamide (**9f**)*

From the reaction of 0.740 g (4-chlorophenyl)(phenyl)methanamine, 1.397 g chloride **8c** and 0.404 g TEA, and after purification by column chromatography (mobile phase cyclohexane/ethyl acetate/methanol 30:10:5) and trituration with ether/petroleum ether, 0.307 g (17%) of **9f** was obtained; mp 158–159.5 ^{o}C; IR (KBr): ν_{max} 3394, 3279, 3062, 1730, 1651, 1492, 1450, 1410, 1381, 1321, 1290, 1219, 1184, 1150, 1093, 1017, 930, 828, 753, 702, 623, 563, 537 cm^{-1}. The structure of product **9f** was confirmed indirectly, by chemical derivatization to compound **10f**.

*4.1.4.7. N-[(4-chlorophenyl)({N'-[(4-methoxyphenyl)(phenyl)methylidene]hydrazinecarbonyl})methyl]-1H-1,2,3-benzotriazole-1-carboxamide (**9g**)*

From the reaction of 0.769 g 4-methoxybenzophenone hydrazone, 1.397 g chloride **8c** and 0.404 g TEA, and after purification by column chromatography (mobile phase cyclohexane/ethyl acetate/methanol 30:10:5) and trituration with ether, 1.136 g (62%) of **9g** was obtained; IR (KBr): ν_{max} 3373, 3307, 3181, 3076, 3049, 2923, 2829, 1733, 1676, 1604, 1506, 1489, 1443,

1377, 1305, 1289, 1256, 1179, 1157, 1108, 1089, 1031, 960, 935, 836, 806, 779, 749, 696, 653, 628, 603, 570, 532 cm^{-1}. The structure of product **9g** was confirmed indirectly, by chemical derivatization to compound **10g**.

*4.1.5. PQ-ureidoamides (**10a-g**): general procedure*

Method A: NaOH solution (*w* = 5%) was added to a solution of 1 mmol PQ diphosphate in water until pH 9-10 was reached, and PQ base was extracted four times with dichloromethane and washed with water until pH 7. The organic layer was dried over anhydrous sodium sulfate, filtered and evaporated under reduced pressure. PQ base and 0.5 mmol Btc-amino acid amide **9** were mixed in dioxane and stirred overnight at room temperature, light protected. The solvent was evaporated under reduced pressure.

Method B: A suspension of 0.4 mmol PQ diphosphate, 0.4 mmol Btc-amino acid amide **9b** and 0.8 mmol TEA in dichloromethane (3 mL) was heated at 70 °C in microwave reactor for 45 min. The solvent was removed under reduced pressure. The residue was dissolved in ethyl acetate/5% NaOH mixture (1:1). The organic layer was extracted with 5% NaOH three times, washed with water two times, dried over anhydrous sodium sulfate, filtered and evaporated.

*4.1.5.1. N-(diphenylmethyl)-2-[({4-[(6-methoxyquinolin-8-yl)amino]pentyl}carbamoyl)amino]-4-methylpentanamide (**10a**)*

Method A, from the reaction of 0.221 g Btc-amino acid amide **9a** and 0.259 g PQ, and after purification by column chromatography (mobile phase cyclohexane/ethyl acetate/methanol 30:10:5) and trituration with ether, 0.253 g (87%) of **10a** was obtained; mp 184.5–185.5 °C; IR (KBr): ν_{max} 3316, 2958, 1655, 1624, 1569, 1519, 1493, 1454, 1422, 1388, 1336, 1290, 1201, 1167, 1155, 1052, 1028, 824, 791, 746, 697 cm^{-1}; ^{1}H NMR (DMSO-d_6) δ 8.89-8.87 (d, *J* = 8.53

Hz, 1H), 8.52 (s, 1H), 8.08-8.06 (d, *J* = 8.25 Hz, 1H), 7.43-7.40 (m, 1H), 7.28-7.20 (m, 10H), 6.46 (s, 1H), 6.25 (s, 1H), 6.12-6.08 (m, 2H), 6.04-6.03 (m, 1H), 5.99-5.97 (d, *J* = 8.60 Hz, 1H), 4.33-4.32 (q, *J* = 8.05 Hz, 14.91 Hz, 1H), 3.81 (s, 3H), 3.60 (m, 1H), 3.00 (m, 2H), 1.61-1.35 (m, 7H), 1.18 (d, *J* = 3.31 Hz, 3H), 0.85-0.82 (m, 6H); ^{13}C NMR (DMSO-d_6) δ 172.46, 159.02, 157.62, 144.64, 144.25, 142.45, 142.40, 134.82, 134.54, 129.60, 128.34, 128.29, 127.45, 127.10, 126.93, 122.12, 96.12, 91.61, 55.73, 55.00, 51.44, 47.05, 42.22, 39.02, 33.53, 26.93, 24.27, 23.03, 22.01, 20.24; ESI-MS: *m/z* calculated for $C_{35}H_{43}N_5O_3$: 581.34, found: 582.2 $(M+1)^+$; Anal. Calcd. for ($C_{35}H_{43}N_5O_3$): C, 72.26; H, 7.45; N, 12.04. Found: C, 72.50; H, 7.47; N, 12.09.

*4.1.5.2. N-(diphenylmethyl)-2-[({4-[(6-methoxyquinolin-8-yl)amino]pentyl}carbamoyl)amino]-N-methyl-2-phenylacetamide (**10b**)*

Method B, from the reaction of 0.190 g Btc-amino acid amide **9b**, 0.182 g PQ diphosphate and 0.081 g TEA, and after purification by column chromatography (mobile phase cyclohexane/ethyl acetate/methanol 30:10:5) and trituration with ether, 0.084 g (34%) of **10b** was obtained; mp 146.5–148.5 °C; IR (KBr): ν_{max} 3335, 3060, 3030, 2962, 2933, 2863, 1622, 1563, 1521, 1495, 1479, 1457, 1406, 1388, 1337, 1308, 1221, 1201, 1163, 1116, 1082, 1052, 1031, 1003, 971, 921, 869, 823, 791, 769, 735, 720, 701, 678, 624, 608, 566, 467 cm^{-1}; ^{1}H NMR (DMSO-d_6) δ 8.54-8.53 (d, *J* = 3.06 Hz, 1H), 8.09-8.07 (d, *J* = 7.94 Hz, 1H, 7.42-7.30 (m, 9H), 7.25 (m, 2H), 7.19-7.13 (m, 3H), 6.96 (s, 1H), 6.89 (m, 1H), 6.67-6.59 (m, 2H), 6.46 (s, 1H), 6.25-6.21 (2s, 2H), 6.12-6.09 (d, *J* = 8.50 Hz, 1H), 5.77-5.75 (d, *J* = 8.11 Hz, 1H), 3.82 (s, 3H), 3.61 (m, 1H), 3.01 (m, 2H), 2.65 (s, 3H), 1.61-1.48 (m, 4H), 1.19-1.18 (d, *J* = 5.83 Hz, 3H); ^{13}C NMR (DMSO-d_6) δ 171.34, 159.00, 157.07, 144.63, 144.24, 138.81, 138.62, 134.80, 134.51, 129.58, 128.66, 128.56, 128.49, 128.38, 128.22, 127.70, 127.36, 122.10, 96.11, 91.62, 60.33, 54.96, 54.26, 47.00, 39.02, 33.52, 31.69, 26.87, 20.21; ESI-MS: *m/z* calculated for $C_{38}H_{41}N_5O_3$: 615.32, found: 616.5

$(M+1)^+$, calculated for $C_{13}H_{10}^{\bullet+}$: 166.08, found: 166.9 ($C_{13}H_{10}^{\bullet+}$); Anal. Calcd. for ($C_{38}H_{41}N_5O_3$): C, 74.12; H, 6.71; N, 11.37. Found: C, 74.39; H, 6.72; N, 11.33.

*4.1.5.3. N-[(4-chlorophenyl)(phenyl)methyl]-2-[({4-[(6-methoxyquinolin-8-yl)amino]pentyl}carbamoyl)amino]-2-phenylacetamide (**10c**)*

Method A, from the reaction of 0.322 g (0.65 mmol) Btc-amino acid amide **9c** and 0.259 g PQ, and after purification by column chromatography (mobile phase cyclohexane/ethyl acetate/methanol 30:10:5) and trituration with ether, 0.351 g (85%) of **10c** was obtained; mp 129–131 °C; IR (KBr): ν_{max} 3317, 3255, 1621, 1571, 1547, 1518, 1489, 1453, 1422, 1386, 1218, 1157, 1090, 1051, 1029, 1014, 818, 790, 697 cm^{-1}; ^1H NMR (DMSO-d_6) δ 9.28-9.25 (dd, J = 5.74 Hz, 8.25 Hz, 1H), 8.54-8.53 (d, J = 4.09 Hz, 1H), 8.09-8.06 (dd, J = 1.41 Hz, 8.27 Hz, 1H), 7.44-7.38 (m, 4H), 7.36-7.16 (m, 9H), 7.13-7.09 (m, 2H), 6.69-6.65 (dd, J = 3.84 Hz, 8.57 Hz, 1H), 6.48 (s, 1H), 6.26-6.24 (2s, 2H), 6.12-6.07 (m, 2H), 5.53-5.50 (dd, J = 5.50 Hz, 8.37 Hz, 1H), 3.82 (s, 3H), 3.61 (m, 1H), 3.01 (m, 2H), 1.61-1.44 (m, 4H), 1.19-1.18 (d, J = 6.25 Hz, 3H); ^{13}C NMR (DMSO-d_6) δ 170.08, 159.01, 157.09, 144.64, 144.26, 141.66, 141.09, 140.25, 134.82, 134.53, 131.75, 129.60, 129.37, 128.75, 128.51, 128.35, 128.21, 127.52, 126.92, 126.58, 122.13, 96.12, 91.63, 56.39, 55.26, 55.00, 47.03, 39.02, 33.52, 26.85, 20.23; ESI-MS: *m/z* calculated for $C_{37}H_{38}ClN_5O_3$: 635.27; found 636.2 $(M+1)^+$; Anal. Calcd. for ($C_{37}H_{38}ClN_5O_3$): C, 69.85; H, 6.02; N, 11.01. Found: C, 69.73; H, 6.00; N, 10.99.

*4.1.5.4. N-(4-bromophenyl)-2-(4-chlorophenyl)-2-[({4-[(6-methoxyquinolin-8-yl)amino]pentyl}carbamoyl)amino]acetamide (**10d**)*

Method A, from the reaction of 0.242 g Btc-amino acid amide **9d** and 0.259 g PQ, and after purification by column chromatography (mobile phase cyclohexane/dichloromethane/methanol 10:18:2 and cyclohexane/ethyl acetate/methanol 30:10:5) and trituration with ether, 0.209 g

(67%) of **10d** was obtained; mp 152–154.5 °C; IR (KBr): ν_{max} 3335, 3285, 3093, 3049, 2961, 2928, 2857, 1635, 1591, 1544, 1517, 1486, 1454, 1421, 1388, 1347, 1303, 1283, 1218, 1201, 1157, 1091, 1072, 1050, 1028, 1009, 968, 935, 899, 817, 787, 760, 710, 674, 622, 551, 499 cm^{-1}; ^{1}H NMR (DMSO-d_6) δ 8.96 (s, 1H), 8.54-8.53 (d, J = 3.87 Hz, 1H), 8.44 (s, 1H), 8.09-8.06 (d, J = 8.20 Hz, 1H), 7.53-7.46 (m, 1H), 7.44-7.36 (m, 6H), 7.33-7.30 (m, 2H), 7.12-7.09 (dd, J = 3.61 Hz, 7.49 Hz, 1H), 6.47 (s, 1H), 6.25 (s, 1H), 6.09-6.06 (d, J = 8.75 Hz, 1H), 5.33-5.30 (d, J = 7.71 Hz, 1H), 3.82 (s, 3H), 3.57 (m, 1H), 3.09 (m, 2H), 1.51-1.40 (m, 4H), 1.15-1.12 (d, J = 5.74 Hz, 3H); ^{13}C NMR (DMSO-d_6) δ 169.47, 158.99, 153.85, 144.62, 144.24, 139.52, 139.15, 134.80, 134.51, 131.42, 131.42, 128.30, 119.36, 129.57, 122.10, 112.52, 96.10, 91.61, 55.72, 54.98, 46.87, 39.02, 33.27, 25.72, 20.16; ESI-MS: *m/z* calculated for $C_{30}H_{34}BrClN_5O_3$: 625.13, found: 626.3 $(M+1)^+$; Anal. Calcd. for ($C_{30}H_{31}BrClN_5O_3$): C, 57.66; H, 5.00; N, 11.21. Found: C, 57.81; H, 5.02; N, 11.23.

*4.1.5.5. 2-(4-Chlorophenyl)-N-(diphenylmethyl)-2-[({4-[(6-methoxyquinolin-8-yl)amino]pentyl}carbamoyl)amino]acetamide (**10e**)*

Method A, from the reaction of 0.230 g Btc-amino acid amide **9e** and 0.259 g PQ, and after purification by column chromatography (mobile phase cyclohexane/ethyl acetate/methanol 30:10:5) and trituration with ether, 0.114 g (36%) of **10e** was obtained; mp 180–183 °C; IR (KBr): ν_{max} 3321, 3254, 1621, 1572, 1547, 1519, 1491, 1455, 1422, 1388, 1348, 1218, 1197, 1159, 1091, 1051, 1030, 1013, 819, 790, 744, 693 cm^{-1}; ^{1}H NMR (DMSO-d_6) δ 9.27-9.25 (d, J = 8.53 Hz, 1H), 8.53-8.52 (d, J = 3.74 Hz, 1H), 8.08-8.06 (dd, J = 1.46 Hz, 8.24 Hz, 1H), 7.43-7.41 (m, 1H), 7.39-7.31 (m, 5H), 7.28-7.21 (m, 5H), 7.18-7.17 (m, 2H), 7.10-7.09 (d, J = 7.51 Hz, 2H), 6.70-6.69 (d, J = 8.53 Hz, 1H), 6.47 (s, 1H), 6.26-6.24 (2s, 2H), 6.11-6.10 (d, J = 8.70 Hz, 1H), 6.06-6.05 (d, J = 8.49 Hz, 1H), 5.54-5.52 (dd, J = 2.55 Hz, 8.52 Hz, 1H), 3.81 (s, 3H),

3.62-3.60 (m, 1H), 3.02-2.97 (m, 2H), 1.64-1.41 (m, 4H), 1.19-1.18 (d, *J* = 5.54 Hz, 3H); ^{13}C NMR (DMSO-d_6) δ 169.49, 158.98, 156.92, 144.61, 144.21, 142.01, 141.86, 139.47, 134.77, 134.49, 131.81, 129.55, 128.39, 128.34, 128.23, 128.09, 127.44, 127.09, 126.90, 126.80, 122.06, 96.06, 91.62, 56.90, 55.70, 54.95, 47.00, 39.02, 33.47, 26.78, 20.18; ESI-MS: *m/z* calculated for $C_{37}H_{38}ClN_5O_3$: 635.27, found: 636.4 $(M+1)^+$; Anal. Calcd. for ($C_{37}H_{38}ClN_5O_3$): C, 69.85; H, 6.02; N, 11.01. Found: C, 69.79; H, 6.01; N, 11.00.

*4.1.5.6. 2-(4-Chlorophenyl)-N-[(4-chlorophenyl)(phenyl)methyl]-2-[({4-[(6-methoxyquinolin-8-yl)amino]pentyl}carbamoyl)amino]acetamide (**10f**)*

Method A, from the reaction of 0.265 g Btc-amino acid amide **9f** and 0.259 g PQ, and after purification by column chromatography (mobile phase cyclohexane/ethyl acetate/methanol 30:10:5) and trituration with ether, 0.127 g (38%) of **10f** was obtained; mp 150–151.5 °C; IR (KBr): ν_{max} 3317, 3252, 1623, 1519, 1489, 1454, 1387, 1218, 1158, 1091, 1051, 1013, 819, 790, 757, 697 cm^{-1}; ^{1}H NMR (DMSO-d_6) δ 9.29-9.28 (d, *J* = 8.62 Hz, 1H), 8.53 (s, 1H), 8.08-8.07 (d, *J* = 7.19 Hz, 1H), 7.43-7.33 (m, 7H), 7.31-7.23 (m, 4H), 7.13-7.09 (m, 2H), 6.71-6.68 (dd, *J* = 4.04 Hz, 8.40 Hz, 1H), 6.47 (s, 1H), 6.26-6.24 (2s, 2H), 6.11-6.10 (d, *J* = 8.66 Hz, 1H), 6.07-6.06 (d, *J* = 8.28 Hz, 1H), 5.53-5.50 (dt, *J* = 2.30 Hz, 8.23 Hz, 1H), 3.81 (s, 3H), 3.61-3.60 (m, 1H), 3.00 (m, 2H), 1.63-1.42 (m, 4H), 1.19-1.18 (d, *J* = 6.22 Hz, 3H); ^{13}C NMR (DMSO-d_6) δ 169.59, 158.98, 156.94, 144.61, 144.21, 141.50, 140.92, 139.32, 134.76, 134.49, 131.81, 131.56, 129.55, 129.27, 128.67, 128.48, 128.35, 128.21, 128.15, 127.42, 126.84, 122.06, 96.08, 91.62, 55.77, 55.34, 54.95, 47.00, 39.02, 33.47, 26.76, 20.18; ESI-MS: *m/z* calculated for $C_{37}H_{37}Cl_2N_5O_3$: 669.23, found: 670.4 $(M+1)^+$; Anal. Calcd. for ($C_{37}H_{37}Cl_2N_5O_3$): C, 66.27; H, 5.56; N, 10.44. Found: C, 66.40; H, 5.58; N, 10.46.

*4.1.5.7. 3-[(4-Chlorophenyl)({N'-[(4-methoxyphenyl)(phenyl)methylidene]hydrazinecarbonyl})methyl]-1-{4-[(6-methoxyquinolin-8-yl)amino]pentyl}urea (**10g**)*

Method A, from the reaction of 0.269 g Btc-amino acid amide **9g** and 0.259 g PQ, and after purification by column chromatography (mobile phase dichloromethane/methanol 95:5 and cyclohexane/ethyl acetate 1:1) and trituration with ether, 0.068 g (20%) of oil product **10g** was obtained; IR (film): ν_{max} 3349, 2930, 1633, 1610, 1555, 1509, 1454, 1421, 1386, 1324, 1304, 1250, 1220, 1201, 1164, 1090, 1029, 959, 819, 790, 772, 697 cm^{-1}; ^{1}H NMR (DMSO-d_6) δ 10.28 (s, 1H), 8.54-8.53 (d, J = 4.08 Hz, 1H), 8.09-8.06 (d, J = 8.20 Hz, 1H), 7.58-7.52 (m, 2H), 7.44-7.24 (m, 8H), 7.17-7.15 (m, 2H), 7.11 (m, 1H), 6.99-6.92 (m, 2H), 6.74-6.71 (d, J = 8.38 Hz, 1H), 6.48 (s, 1H), 6.27-6.21 (m, 2H), 6.13-6.10 (d, J = 8.71 Hz, 1H), 5.54-5.51 (d, J = 7.95 Hz, 0.63H), 5.37-5.35 (d, J = 7.81 Hz, 0.37H), 3.82 (s, 3H), 3.86-3.84 (d, J = 4.06 Hz, 1H), 3.78-3.76 (d, J = 5.04 Hz, 2H), 3.61 (m, 1H), 3.0 (m, 2H), 1.65-1.48 (m, 4H), 1.21-1.19 (d, J = 6.05 Hz, 3H); ^{13}C NMR (DMSO-d_6) δ 169.45, 167.10, 158.99, 157.00, 155.00, 144.62, 144.24, 138.90, 134.79, 134.51, 132.50, 131.98, 130.17, 129.31, 129.15, 129.06, 128.47, 128.26, 127.65, 129.57, 124.27, 122.09, 114.60, 113.77, 96.09, 91.62, 55.21, 54.97, 47.0, 39.02, 33.48, 26.78, 20.20; ESI-MS: *m/z* calculated for $C_{38}H_{39}ClN_6O_4$: 678.27, found: 679.3 $(M+1)^+$; Anal. Calcd. for ($C_{38}H_{39}ClN_6O_4$): C, 67.20; H, 5.79; N, 12.37. Found: C, 67.39; H, 5.80; N, 12.40.

4.2. Biological evaluation

4.2.1. Activity against erythrocytic stage of P. falciparum

In vitro activity against erythrocytic stages of drug sensitive *P. falciparum* NF54 strain was determined using a ^{3}H-hypoxanthine incorporation assay [46–48]. Compounds were dissolved in

DMSO at 10 mg/ml and added to parasite cultures incubated in RPMI 1640 medium without hypoxanthine, supplemented with HEPES (5.94 g/l), $NaHCO_3$ (2.1 g/l), neomycin (100 U/ml), Albumax® (5 g/l) and washed human red cells A^+ at 2.5% hematocrit (0.3% parasitemia). Serial drug dilutions of eleven 3-fold dilution steps covering a range from 100 to 0.002 µg/ml were prepared. The 96-well plates were incubated in a humidified atmosphere at 37 °C; 4% CO_2, 3% O_2, 93% N_2. After 48 h 50 µl of ^{3}H-hypoxanthine (0.5 µCi) was added to each well of the plate. The plates were incubated for a further 24 h under the same conditions. The plates were then harvested with a Betaplate™ cell harvester (Wallac, Switzerland), and the red blood cells transferred onto a glass fiber filter then washed with distilled water. The dried filters were inserted into a plastic foil with 10 ml of scintillation fluid, and counted in a Betaplate™ liquid scintillation counter (Wallac). IC_{50} values were calculated from sigmoidal inhibition curves by linear interpolation between two neighboring points [49] using Microsoft Excel; see section 4.2.3 below for details and Supplementary Figure S2 for example dose-response curves.

4.2.2. In vitro cytotoxicity on rat L6 primary cells

Assays were performed in 96-well microtiter plates, each well containing 100 µl of RPMI 1640 medium supplemented with 1% L-glutamine (200 mM) and 10% foetal bovine serum, and 4000 L6 cells (a primary cell line derived from rat skeletal myoblasts) [50,51]. Serial drug dilutions of eleven 3-fold dilution steps covering a range from 100 to 0.002 µg/ml were prepared. After 70 hours of incubation the plates were inspected under an inverted microscope to assure growth of the controls and sterile conditions. 10 µl of Alamar Blue was then added to each well and the plates incubated for another 2 hours. Then the plates were read with a microplate fluorometer using an excitation wave length of 536 nm and an emission wave length of 588 nm. The IC_{50}

values were calculated by linear interpolation from the sigmoid dose inhibition curves [49] using SoftmaxPro software (Molecular Devices Cooperation, USA); see section 4.2.3 below for details.

4.2.3. Antiproliferative activity on human cell lines

The experiments were carried out on eight human cell lines, derived from different tissues-of-origin: H460 (lung carcinoma), SW620 (colon carcinoma), MCF-7 (breast adenocarcinoma), A2780 (ovarian endometroid adenocarcinoma), HCT 116 (colorectal carcinoma), HL-60 (acute promyelocytic leukemia), K562 (chronic myeloid leukemia) and Capan-1 (pancreatic adenocarcinoma). Cells were grown in DMEM or RPMI-1640 media with the addition of 10% fetal bovine serum (FBS), 2 mM L-glutamine, 100 U/ml penicillin and 100 µg/ml streptomycin, and cultured as monolayers at 37 °C in a humidified atmosphere with 5% CO_2.

Cells were seeded at 2 $\times 10^4$ to 4 $\times$ 10^4 cells/well (depending on the doubling time of a specific cell line) in a standard 96-well microtiter plates and left to attach for 24 h. Next day, test compounds were added in five serial 10-fold dilutions alone or in combination with 6-aminonicotinamide (always at 10 µM). Working dilutions were freshly prepared on the day of testing. The final concentration of DMSO was <0.2% which was non-toxic to cells. The cell growth rate was evaluated after 72 hours of incubation, using the MTT assay. The percentage of growth (PG) of the cell lines was calculated as described previously [34].

The IC_{50} values for each compound were calculated from concentration-response curves using linear regression analysis by fitting to the two concentrations that give PG values above and below the respective reference value (i.e. 50% growth inhibition). In effect, this is a linear interpolation between the concentration points adjacent to the IC_{50}. We examined to what extent

the IC_{50} values estimated thusly match those found by fitting a non-linear logistic (Hill) equation. This revealed a strong agreement, for instance, the average difference of IC_{50} calculated by the two methods for compounds **3b**, **5v**, **10e** and **10f** (considering antimalarial activity and antiproliferative activity over H460 and MCF-7 cell lines) is 0.06 µM units; the dose-response curves obtained with both methods of fitting are shown in Supporting Figure S2. This agreement is consistent with past recommendations to use the linear interpolation approach for finding IC_{50} in sigmoidal drug response curves [49]. Each test point was performed in four technical replicates. The data reported for H460, MCF-7, SW620 and A2780 cells in Table 2 were measured in at least two separate experiments (biological replicates), while the data for an extended set of cell lines (HCT 116, HL-60, K562 and Capan-1) in Supporting Table S1 represent measurements from a single experiment.

4.3. QSAR modeling

4.3.1. Collection and pre-processing of PQ derivatives and antimalarial activity

The QSAR model for prediction of antimalarial activity (log IC_{50} against *P. falciparum* NF54 strain) was trained using the Support Vector Machines (SVM) algorithm for regression (henceforth: support vector regression), as implemented in the LIBSVM software [52]. In this study, SVM models were trained on a set of 56 compounds (structures provided in Supporting Data) represented with 2D molecular descriptors calculated with Chemistry Development Kit (CDK) [53]. A set of 285 CDK descriptors were initially calculated, followed by the removal of descriptors with constant or missing values for all compounds, yielding 140 descriptors in total. Prior to calculation of the CDK molecular descriptors, structures were represented as SMILES

strings and preprocessed using the Instant JChem Standardizer (with *Remove fragment, Neutralize, Remove explicit hydrogens,* and *Dearomatize* options) [54].

Out of 56 compounds in the training set, synthesis of 23 compounds were reported in our previous work [23–26], while their antimalarial activity is reported in the current paper (Table 1). Of note, we required at least two independent experimental measurements of antimalarial activity to include the compound in our QSAR data series, therefore excluding four compounds at this stage (**2i**, **5c**, **5q** and **5s**); all other compounds were measured in two or three experiments (three technical replicates each).

An additional 33 compounds and the corresponding antimalarial activity measurements were collected from the studies of Kaur *et al*. [37–39]. Out of 88 reported compounds in total, we selected the ones occupying similar chemical space to our compounds, as determined by Principal Component Analysis (PCA); bounding box on principal components 1 and 2 is shown in Figure S3. Among the compounds of Kaur *et al*., there are several stereoisomers which cannot be differentiated with 2D CDK molecular descriptors we used, therefore, we collapsed such stereoisomers into a single molecule (without stereochemistry) whose antimalarial activity was set to the mean activity of the stereoisomers. The PCA bounding box filtering and unification of stereoisomers yielded total of 33 compounds. The antimalarial activity of our compounds was measured against the *P. falciparum* NF54 strain (as described in 2.2.1), while Kaur *et al*. reported antimalarial activity against two strains of *P. falciparum* (D6 and W2) and we used the mean activity (log IC_{50}) across these two strains, which is very highly correlated between the strains (R^2=0.931 across the Kaur *et al*. compounds). To ensure compatibility of log IC_{50} values, the activities of compounds reported by Kaur *et al*. were converted to molar concentrations;

following that, the salts were removed from compound molecular structures prior to calculating the molecular descriptors.

4.3.2. Using support vector machines regression to prioritize candidate compounds

As recommended by LIBSVM authors, the radial basis function (RBF, or Gaussian) kernel was used and the regularization parameters were optimized in a grid search procedure (C from 2^{-5}, 2^{-4}, …, 2^{20} and γ from 2^{-15}, 2^{-14}, …, 2^{5}) [55]. The models were evaluated by using 10-fold cross validation which was repeated 10 times with different random initialization. The model with the highest R^2, having R^2 = 0.785 and RMSE = 0.284 was obtained for C = 2^5 and γ = 2^{-9}, however we retained the model with very similar predictive performance (R^2 = 0.776, RMSE = 0.294; Figure 2a), but more favorable parameter settings (C = 2^1 and γ = 2^{-6}) for further prediction. Namely, lower values of the SVM regularization parameters C and γ are known to result in simpler, more parsimonious models (typically evident in less non-linearity and in a smaller number of support vectors), which are less likely to overfit to training data, thus generalizing better to unseen compounds. To estimate the predictive ability on out-of-sample data, the predictions of the SVM model were evaluated against an independent set of 37 compounds whose antimalarial activity was experimentally determined in this work post-QSAR analysis (Tables 1 and S2, compounds **1a-k**, **2h**, **4a-k**, **5i-m**, **5p**, **5r**; compounds were originally reported in references [26,28,29], and additionally the novel compounds **10a-g** reported here, see below), showing agreement with the measured activities (R^2 = 0.423, RMSE = 0.403; Figure 2b). The model was applied to infer the antimalarial activity of an in-house virtual library of 522 compounds (structures provided in Supporting Data) in order to prioritize chemical synthesis of novel PQ derivatives **10a-g**. Given the strong predicted antimalarial activity (Figure 2c),

ureidoamides **10a-g** were selected for synthesis and evaluation for activity against *P. falciparum* and toxicity to mammalian cell lines.

4.3.3. Predicting antimalarial activity for a comprehensive set of PQ-like compounds

Further, we aimed to create a comprehensive QSAR model, therefore supplementing the initial training set of 56 compounds with the 37 additional PQ-related compounds (see above). After repeating the same SVM training and parameter optimization procedure on these 93 compounds, we obtained an accurate regression model (cross-validation R^2 = 0.729, RMSE = 0.312; while using parameters C = 2^5, γ = 2^{-7}). The updated 93-compound SVM model was then applied to predict the antimalarial activity of a large set of compounds extracted from PubChem database [56] (Supporting Information) that were within the applicability domain of our model. We ensured this in the following manner: for each compound from the training set, we extracted compounds from PubChem similar to it (querying for Tanimoto score $\geq$ 0.85, via the PubChem API; duplicates were excluded). Furthermore, the compounds were projected to the same PC coordinates as reported in Figure S3 and filtered using the same PCA bounding box approach, yielding 13 401 compounds in total. In addition to predictions of antimalarial activity for these 13 401 compounds, we also provide predictions of their cytotoxicity based on cell line screening data (Supporting Information; Figure S1); see below for details.

To develop a model for prediction of cytotoxicity, the NCI-60 cancer cell line screening database was used [57]. As a measure of cytotoxicity, we used the median of compound's activities (expressed as –log IC_{50}) across the 60 cell lines. We considered only compounds with median > 4 (i.e., a value assigned if no activity was detected with maximal concentration tested for a given compound). Furthermore, to ensure the applicability of the cytotoxicity model to our data, only

compounds from NCI-60 that are close in chemical space to our compounds were considered. To this end, for each molecule from our dataset, its k nearest neighbors in NCI-60 were selected (excluding identical molecules), considering $k \in \{20,50,75,100\}$. For the final model, $k = 75$ was used since it yielded the best cross-validation performance ($R^2 = 0.514$), resulting in 9301 compounds in total. Compounds were represented with 2D CDK molecular descriptors and SVM model was trained following the same procedure as described above.

To select the most important molecular descriptors in prediction of antimalarial activity, we used a forward feature selection scheme employing an SVM. The full data set containing 140 CDK descriptors was divided into data sets containing single descriptors and evaluated according to the cross-validation scheme as described above. The Pearson correlation coefficient was a measure of relevance for the descriptor. Top 15 descriptors obtained in this way are reported in Figure S4, while the complete list is provided in Table S2.

The schematic representation of the QSAR modeling pipeline of this study is reported in Supporting Figure S5.

Supporting information. The Supporting Information and Supporting Data are available via the journal website.

Supporting Information: A comprehensive QSAR model for antimalarial activity and cytotoxicity of PQ-like compounds; IC_{50} values for HCT 116, HL-60, K562 and Capan-1 human cell lines; Plot of the antimalarial activity and cytotoxicity for 13 401 compounds extracted from the PubChem database; Comparison of the growth inhibition curves fitted with non-linear logistic regression and linear interpolation; Plot of the first two principal component of PCA analysis performed on 2D CDK molecular descriptors of the compounds reported by our group

and compounds collected from the studies of Kaur et al; The 15 most informative single descriptors for antimalarial activity prediction in a SVM model; The cross-validation performance of individual CDK descriptors in a forward feature selection scheme employing SVM; The schematic representation of the QSAR modeling pipeline; Analytical and spectral data of the prepared compounds; ^{1}H and ^{13}C NMR spectra of the prepared compounds; Copies of IR, ^{1}H and ^{13}C NMR, and MS spectra of new compounds; Atom assignation of compounds **7c**, **9a-g** and **10a-g** (PDF).

Supporting Data: SMILES codes for all compounds: SVM training set (56 compounds); In house library (522 compounds); Compounds from PubChem predicted to be more active and less toxic than primaquine (199 compounds); Complete list of primaquine-like compounds retrieved from PubChem (13 401 compounds) (XLSX).

Acknowledgment

We acknowledge the financial support of Croatian Science Foundation via projects IP-09-2014-1501 ("PVSderivatives") to BZ and IP-2013-5660 ("MultiCaST") to MK. FS and JL are supported by IRB Barcelona core funding, ERC StG 757700 ("HYPER-INSIGHT") and the Ramon y Cajal fellowship of the Spanish Ministry of Economy, Industry and Competitiveness. We sincerely thank Prof. Dominique Schols for a part of cytostatic activity evaluation (Table S1).

Abbreviations

6-AN, 6-aminonicotinamide; AD, applicability domain; CDK, chemistry development kit; ESI, electron spray ionization; FBS, fetal bovine serum; G6PD, glucose-6-phosphate dehydrogenase;

IC_{50}, the concentration of the tested compound necessary for 50% growth inhibition; PCA, principal component analysis; PG, percentage of growth; PQ, primaquine; QSAR, quantitative-structure activity relationship; RMSE, root mean squared error; SI, selectivity index; SMP3, Stuart Melting Point; SVM, support vector machines.

References

[1] World Malaria Report 2016, (2016). http://www.who.int/malaria/publications/world-malaria-report-2016/report/en/ (accessed January 14, 2018).

[2] T.L. Lemke, D.A. Williams, V.F. Roche, S.W. Zito, Foye's principles of medicinal chemistry, 6th ed., Wolters Kluwer (Health)/Lippincott Williams & Wilkins, Philadelphia, 2008.

[3] L. Tilley, P. Loria, M. Foley, Chloroquine and other ouinoline antimalarials, in: Antimalar. Chemother. Mech. Action Resist. New Dir. Drug Discov., Humana Press, Totowa, NJ, 2001.

[4] N.J. White, Primaquine to prevent transmission of falciparum malaria, Lancet Infect. Dis. 13 (2013) 175–181.

[5] L. Luzzatto, G. Battistuzzi, Glucose-6-Phosphate Dehydrogenase, in: Adv. Hum. Genet. 14, Springer, Boston, MA, 1985: pp. 217–329.

[6] E.T. Nkhoma, C. Poole, V. Vannappagari, S.A. Hall, E. Beutler, The global prevalence of glucose-6-phosphate dehydrogenase deficiency: A systematic review and meta-analysis, Blood Cells. Mol. Dis. 42 (2009) 267–278.

[7] N.J. White, L.G. Qiao, G. Qi, L. Luzzatto, Rationale for recommending a lower dose of primaquine as a Plasmodium falciparum gametocytocide in populations where G6PD deficiency is common, Malar. J. 11 (2012) 418.

[8] A.L. Peters, C.J.F. Van Noorden, Glucose-6-phosphate Dehydrogenase Deficiency and Malaria: Cytochemical Detection of Heterozygous G6PD Deficiency in Women, J. Histochem. Cytochem. 57 (2009) 1003–1011.

[9] M. Jain, S. Vangapandu, S. Sachdeva, S. Singh, P.P. Singh, G.B. Jena, K. Tikoo, P. Ramarao, C.L. Kaul, R. Jain, Discovery of a bulky 2-tert-butyl group containing primaquine analogue that exhibits potent blood-schizontocidal antimalarial activities and complete elimination of methemoglobin toxicity, J. Med. Chem. 47 (2004) 285–287.

[10] P. Gomes, M.J. Araújo, M. Rodrigues, N. Vale, Z. Azevedo, J. Iley, P. Chambel, J. Morais, R. Moreira, Synthesis of imidazolidin-4-one and 1H-imidazo[2,1-a]isoindole-2,5(3H,9bH)-dione derivatives of primaquine: scope and limitations, Tetrahedron. 60 (2004) 5551–5562.

[11] P. Chambel, R. Capela, F. Lopes, J. Iley, J. Morais, L. Gouveia, J.R.B. Gomes, P. Gomes, R. Moreira, Reactivity of imidazolidin-4-one derivatives of primaquine: implications for prodrug design, Tetrahedron. 62 (2006) 9883–9891.

[12] N. Vale, M.S. Collins, J. Gut, R. Ferraz, P.J. Rosenthal, M.T. Cushion, R. Moreira, P. Gomes, Anti-Pneumocystis carinii and antiplasmodial activities of primaquine-derived imidazolidin-4-ones, Bioorg. Med. Chem. Lett. 18 (2008) 485–488.

[13] C. Sall, A.-D. Yapi, N. Desbois, S. Chevalley, J.-M. Chezal, K. Tan, J.-C. Teulade, A. Valentin, Y. Blache, Design, synthesis, and biological activities of conformationally restricted analogs of primaquine with a 1,10-phenanthroline framework, Bioorg. Med. Chem. Lett. 18 (2008) 4666–4669.

[14] N. Vale, J. Matos, R. Moreira, P. Gomes, Amino acids as selective acylating agents: regioselective N1-acylation of imidazolidin-4-one derivatives of the antimalarial drug primaquine, Tetrahedron. 64 (2008) 11144–11149.

[15] N. Vale, J. Matos, J. Gut, F. Nogueira, V. do Rosário, P.J. Rosenthal, R. Moreira, P. Gomes, Imidazolidin-4-one peptidomimetic derivatives of primaquine: synthesis and antimalarial activity, Bioorg. Med. Chem. Lett. 18 (2008) 4150–4153.

[16] N. Vale, F. Nogueira, V.E. do Rosário, P. Gomes, R. Moreira, Primaquine dipeptide derivatives bearing an imidazolidin-4-one moiety at the N-terminus as potential antimalarial prodrugs, Eur. J. Med. Chem. 44 (2009) 2506–2516. doi:10.1016/j.ejmech.2009.01.018.

[17] N. Vale, R. Moreira, P. Gomes, Primaquine revisited six decades after its discovery, Eur. J. Med. Chem. 44 (2009) 937–953.

[18] R. Capela, G.G. Cabal, P.J. Rosenthal, J. Gut, M.M. Mota, R. Moreira, F. Lopes, M. Prudêncio, Design and evaluation of primaquine-artemisinin hybrids as a multistage antimalarial strategy, Antimicrob. Agents Chemother. 55 (2011) 4698–4706.

[19] B. Pérez, C. Teixeira, I.S. Albuquerque, J. Gut, P.J. Rosenthal, M. Prudêncio, P. Gomes, PRIMACINS, N-cinnamoyl-primaquine conjugates, with improved liver-stage antimalarial activity, MedChemComm. 3 (2012) 1170–1172.

[20] G. Mata, V.E. do Rosário, J. Iley, L. Constantino, R. Moreira, A carbamate-based approach to primaquine prodrugs: Antimalarial activity, chemical stability and enzymatic activation, Bioorg. Med. Chem. 20 (2012) 886–892.

[21] A. Gomes, M. Machado, L. Lobo, F. Nogueira, M. Prudêncio, C. Teixeira, P. Gomes, N-cinnamoylation of antimalarial classics: effects of using acyl groups other than cinnamoyl toward dual-stage antimalarials, ChemMedChem. 10 (2015) 1344–1349.

[22] H. Kaur, M. Machado, C. de Kock, P. Smith, K. Chibale, M. Prudêncio, K. Singh, Primaquine–pyrimidine hybrids: synthesis and dual-stage antiplasmodial activity, Eur. J. Med. Chem. 101 (2015) 266–273.

[23] G. Džimbeg, B. Zorc, M. Kralj, K. Ester, K. Pavelić, G. Andrei, R. Snoeck, J. Balzarini, E. De Clercq, M. Mintas, The novel primaquine derivatives of N-alkyl, cycloalkyl or aryl urea: Synthesis, cytostatic and antiviral activity evaluations, Eur. J. Med. Chem. 43 (2008) 1180–1187.

[24] M. Šimunović, I. Perković, B. Zorc, K. Ester, M. Kralj, D. Hadjipavlou-Litina, E. Pontiki, Urea and carbamate derivatives of primaquine: Synthesis, cytostatic and antioxidant activities, Bioorg. Med. Chem. 17 (2009) 5605–5613.

[25] I. Perković, S. Tršinar, J. Žanetić, M. Kralj, I. Martin-Kleiner, J. Balzarini, D. Hadjipavlou-Litina, A.M. Katsori, B. Zorc, Novel 1-acyl-4-substituted semicarbazide derivatives of primaquine − synthesis, cytostatic, antiviral and antioxidative studies, J. Enzyme Inhib. Med. Chem. 28 (2012) 601–610.

[26] K. Pavić, I. Perković, M. Cindrić, M. Pranjić, I. Martin-Kleiner, M. Kralj, D. Schols, D. Hadjipavlou-Litina, A.-M. Katsori, B. Zorc, Novel semicarbazides and ureas of primaquine with bulky aryl or hydroxyalkyl substituents: Synthesis, cytostatic and antioxidative activity, Eur. J. Med. Chem. 86 (2014) 502–514.

[27] E. Kedzierska, J. Orzelska, I. Perković, D. Knežević, S. Fidecka, M. Kaiser, B. Zorc, Pharmacological effects of primaquine ureas and semicarbazides on the central nervous system in mice and antimalarial activity in vitro, Fundam. Clin. Pharmacol. 30 (2016) 58–69.

[28] I. Perković, M. Antunović, I. Marijanović, K. Pavić, K. Ester, M. Kralj, J. Vlainić, I. Kosalec, D. Schols, D. Hadjipavlou-Litina, E. Pontiki, B. Zorc, Novel urea and bis-urea primaquine derivatives with hydroxyphenyl or halogenphenyl substituents: synthesis and biological evaluation, Eur. J. Med. Chem. 124 (2016) 622–636.

[29] K. Pavić, I. Perković, P. Gilja, F. Kozlina, K. Ester, M. Kralj, D. Schols, D. Hadjipavlou-Litina, E. Pontiki, B. Zorc, Design, synthesis and biological evaluation of novel primaquine-cinnamic acid conjugates of the amide and acylsemicarbazide type, Molecules. 21 (2016) 1629–1653.

[30] I. Perković, I. Butula, Z. Rajić, D. Hadjipavlou-Litina, E. Pontiki, B. Zorc, Novel ureidoamides derived from amino acids: synthesis and preliminary biological screening, Croat. Chem. Acta. 83 (2010) 151–161.

[31] I. Perković, I. Butula, B. Zorc, K. Hock, S.K. Pavelić, K. Pavelić, E.D. Clercq, J. Balzarini, M. Mintas, Novel lipophilic hydroxyurea derivatives: synthesis, cytostatic and antiviral activity evaluations, Chem. Biol. Drug Des. 71 (2008) 546–553.

[32] I. Butula, B. Zorc, V. Vela, Reactions with N-benzotriazolecarbonyl chloride. VII. Reactions with amino acids, Croat. Chem. Acta. 54 (1981) 435–440.

[33] O. Ivanciuc, Applications of Support Vector Machines in Chemistry, in: K.B. Lipkowitz, T.R. Cundari (Eds.), Rev. Comput. Chem., John Wiley & Sons, Inc., 2007: pp. 291–400.

[34] J. Levatić, J. Ćurak, M. Kralj, T. Šmuc, M. Osmak, F. Supek, Accurate Models for P-gp Drug Recognition Induced from a Cancer Cell Line Cytotoxicity Screen, J. Med. Chem. 54 (2013) 5691-5708.

[35] M. Gredičak, F. Supek, M. Kralj, Z. Majer, M. Hollósi, T. Šmuc, K. Mlinarić-Majerski, Š. Horvat, Computational structure–activity study directs synthesis of novel antitumor enkephalin analogs, Amino Acids. 38 (2010) 1185–1191.

[36] F. Supek, T.Š. Ramljak, M. Marjanović, M. Buljubašić, G. Kragol, N. Ilić, T. Šmuc, D. Zahradka, K. Mlinarić-Majerski, M. Kralj, Could LogP be a principal determinant of biological activity in 18-crown-6 ethers? Synthesis of biologically active adamantane-substituted diaza-crowns, Eur. J. Med. Chem. 46 (2011) 3444–3454.

[37] K. Kaur, M. Jain, S.I. Khan, M.R. Jacob, B.L. Tekwani, S. Singh, P.P. Singh, R. Jain, Synthesis, antiprotozoal, antimicrobial, β-hematin inhibition, cytotoxicity and methemoglobin (MetHb) formation activities of bis(8-aminoquinolines), Bioorg. Med. Chem. 19 (2011) 197–210.

[38] K. Kaur, M. Jain, S. I. Khan, M. R. Jacob, B. L. Tekwani, S. Singh, P. Pal Singh, R. Jain, Extended side chain analogues of 8-aminoquinolines: Synthesis and evaluation of antiprotozoal, antimicrobial, β-hematin inhibition, and cytotoxic activities, MedChemComm. 2 (2011) 300–307.

[39] K. Kaur, M. Jain, S.I. Khan, M.R. Jacob, B.L. Tekwani, S. Singh, P.P. Singh, R. Jain, Amino acid, dipeptide and pseudodipeptide conjugates of ring-substituted 8-aminoquinolines: synthesis and evaluation of anti-infective, β-haematin inhibition and cytotoxic activities, Eur. J. Med. Chem. 52 (2012) 230–241.

[40] J. Watson, W.R. Taylor, D. Menard, S. Kheng, N.J. White, Modelling primaquine-induced haemolysis in G6PD deficiency, ELife. 6 (2017) e23061.

[41] K. Baird, Origins and implications of neglect of G6PD deficiency and primaquine toxicity in Plasmodium vivax malaria, Pathog. Glob. Health. 109 (2015) 93–106.

[42] I. Butula, M. Prostenik, V. Vela, Reactions with 1-benzotriazolecarboxylic acid chloride. 1. Synthesis of 2, 6-bis (hydroxymethyl) pyridinedicarbamates, Croat. Chem. Acta. 49 (1977) 837–842.

[43] I. Butula, M. Jadrijević-Mladar Takač, Reactions with 1-benzotriazolecarboxylic acid chloride. VIII. Synthesis of *N*-hydroxyisocyanate derivatives, Croat. Chem. Acta. 73 (2000) 569–574.

[44] G.R. Newkome, D.L. Fishel, Preparation of hydrazones: acetophenone ydrazone, Org. Synth. (1970) 102–103.

[45] N. Opačić, M. Barbarić, B. Zorc, M. Cetina, A. Nagl, D. Frković, M. Kralj, K. Pavelić, J. Balzarini, G. Andrei, R. Snoeck, E. De Clercq, S. Raić-Malić, M. Mintas, The novel L- and D-amino acid derivatives of hydroxyurea and hydantoins: synthesis, X-ray crystal structure study, and cytostatic and antiviral activity evaluations, J. Med. Chem. 48 (2005) 475–482.

[46] R.E. Desjardins, C.J. Canfield, J.D. Haynes, J.D. Chulay, Quantitative assessment of antimalarial activity in vitro by a semiautomated microdilution technique., Antimicrob. Agents Chemother. 16 (1979) 710–718.

[47] H. Matile, J.R.L. Pink, Plasmodium falciparum malaria parasite cultures and their use in immunology, Academic Press, San Diego, 1990.

[48] T. Ponnudurai, A.D. Leeuwenberg, J.H. Meuwissen, Chloroquine sensitivity of isolates of Plasmodium falciparum adapted to in vitro culture., Trop. Geogr. Med. 33 (1981) 50–54.

[49] W. Huber, J.C. Koella, A comparison of three methods of estimating EC50 in studies of drug resistance of malaria parasites, Acta Trop. 55 (1993) 257–261.

[50] B. Page, M. Page, C. Noel, A new fluorometric assay for cytotoxicity measurements in-vitro, Int. J. Oncol. 3 (1993) 473–476.

[51] S. Ansar Ahmed, R.M. Gogal, J.E. Walsh, A new rapid and simple non-radioactive assay to monitor and determine the proliferation of lymphocytes: an alternative to [3H]thymidine incorporation assay, J. Immunol. Methods. 170 (1994) 211–224.

[52] C.-C. Chang, C.-J. Lin, LIBSVM: A library for support vector machines, ACM Trans. Intell. Syst. Technol. 2 (2011) 27:1–27:27.

[53] C. Steinbeck, Y. Han, S. Kuhn, O. Horlacher, E. Luttmann, E. Willighagen, The Chemistry Development Kit (CDK): An Open-Source Java Library for Chemo- and Bioinformatics, J. Chem. Inf. Comput. Sci. 43 (2003) 493–500.

[54] Instant JChem 17.24.0, ChemAxon, 2017.

[55] C.-W. Hsu, C.-C. Chang, L. Chih-Jen, A Practical Guide to Support Vector Classification, (2010).

[56] S. Kim, P.A. Thiessen, E.E. Bolton, J. Chen, G. Fu, A. Gindulyte, L. Han, J. He, S. He, B.A. Shoemaker, J. Wang, B. Yu, J. Zhang, S.H. Bryant, PubChem substance and compound databases, Nucleic Acids Res. 44 (2016) D1202–D1213.

[57] R.H. Shoemaker, The NCI60 human tumour cell line anticancer drug screen, Nat. Rev. Cancer. 6 (2006) 813–823.

Graphical abstract

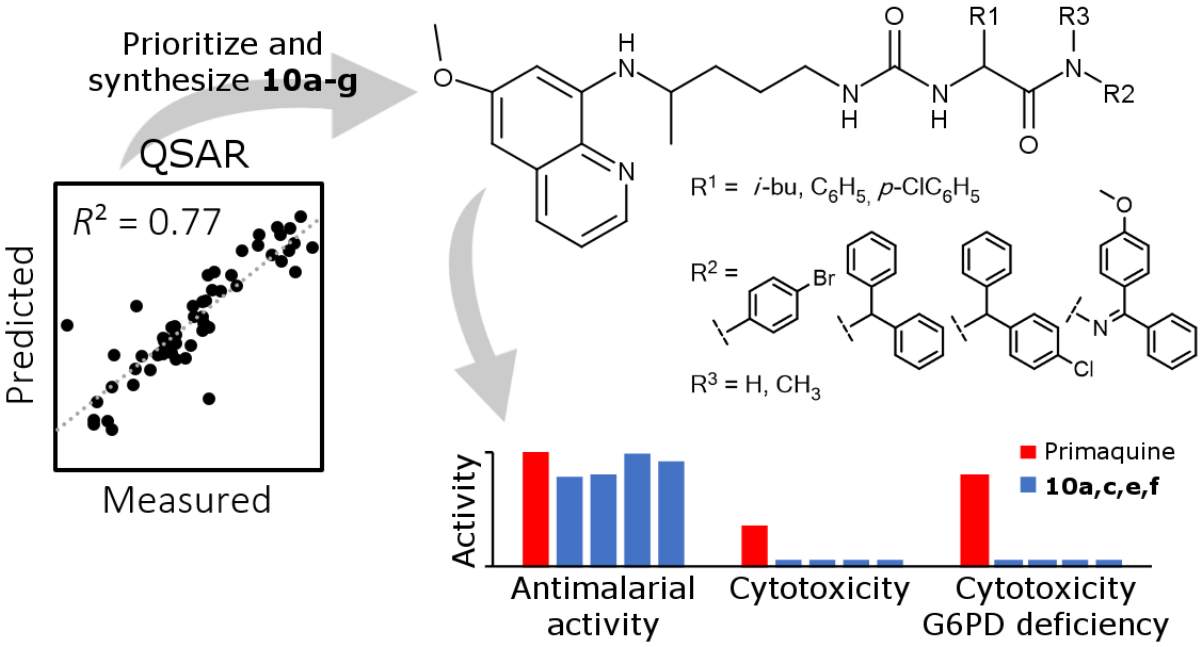

Highlights

- Trityl and methoxybenzhydryl primaquine (PQ) derivatives have activity against *Plasmodium*
- QSAR model based on Support Vector Machines predicts activity with R^2 = 0.776
- Novel PQ-ureidoamides are active, but an order of magnitude less cytotoxic *in vitro* than PQ
- Low toxicity is retained in G6PD-inhibited conditions, unlike previous PQ compounds